Addis Ababa University

Addis Ababa Institute of Technology

School of Mechanical and Industrial Engineering

Analyze the Influence of Train Overloading on Wheel Surface Damage in AALRT

A Thesis Submitted to the Graduate School of Mechanical and Industrial Engineering in Partial Fulfillment of the Requirements for the Degree of Masters of Science in Railway Mechanical Engineering

Submitted by: Yoseph Yaekob

Advisor: Mr. Habtamu Tkubet

June 2017

Addis Ababa University

Addis Ababa Institute of Technology

School of Mechanical and Industrial Engineering

This is to certify that the thesis prepared by Yoseph Yaekob, entitled: *Analyze the Influence of Train Overloading on Wheel Surface Damage in AALRT* and submitted in partial fulfillment of the requirements for the degree of Master of Science (Mechanical and Industrial Engineering) complies with the regulations of the University and meets the accepted standards with respect to originality and quality.

Approved By board of Examiners:

Mr. Habtamu Tkubet	_____	_____
(Advisor)	Signature	Date
_____	_____	_____
(Railway center head)	Signature	Date
_____	_____	_____
(Internal Examiner)	Signature	Date
_____	_____	_____
(External Examiner)	Signature	Date

Acknowledgement

First of all, I would like to thank the almighty God, helps me to finish this thesis from the beginning to final. Next I would like to thank my advisor Mr. Habtamu Tkubet for his valuable guidance and support. I would also like to thank staffs of Ethiopian Railways Corporation in AALRT for providing me with the necessary data which are used in the development of the thesis. I am also grateful to my friends and classmates who have been very cooperative and supportive with different materials and ideas. Finally, thanks to my family for their support, motivation and encouragement.

Abstract

Stress in Railway transportation systems results usually on the contact area between wheel and rail. These high stress which presents on the contact point results damage on the wheel. Damage in railway is resulting from contact between wheel and rail; and a variety of changes to the wheel that may reduce serviceability.

The damage assessment in wheel-rail contact is a very complex problem, as is affected by many parameters (materials, load history, climatic condition and others) and different damage mechanisms can occur. The main objective of this research deals with Analyze the Influence of Train Overloading on Wheel Surface Damage in the case of AALRT. The contacts of wheel and rail in straight track are a non-conformal contact which is between wheels tread and rail head. The analysis is done using hertz wheel rail contact theory; and also modeled and analyzed using CATIA and ANSYS software. The materials of the wheels have different mechanical properties but the same structural dimensions and profiles.

Deformation, stress, fatigue life and fatigue damage of wheels are analyzed using ANSYS and different results on the wheel materials are observed. Deformation and stress on the wheel increases due to the increment of applied load and these results high fatigue damage on the wheel and decrease materials fatigue life. The fatigue life (76,262) of CL60 wheels are less with high deformation and damage (13,113) compared with R8T and ER7 (fatigue life (123,140) and damage (8,120.7)) wheel materials.

As observed from the results ER7 wheel have long life with less deformation and damage than other wheel materials CL60 and R8T wheels. And it may provide improved performances, minimize the sensitivity of overloading and can provide longer life.

Key words: wheel-rail contact, wheel-rail materials, overloading, ANSYS.

Table of Contents

List of Figures

List of Tables

Nomenclatures

AALRT:	Addis Ababa Light Rail Transit
AAR:	Association of American Railroad
AW:	Carrying Capacity (Working Condition)
AW0:	Empty Weight
AW3:	Maximum Permissible Weight
A and B:	Positive Constants
a:	Major (Forward) Semi-Axis
BS:	Britain Standard
b:	Minor (Lateral) Semi-Axis
ERC:	Ethiopian Railway Corporation
E:	Elastic Module
Ew:	Wheel Material Elastic Module
Er:	Rail Material Elastic Module
EN:	European Railroad Standard
FE:	Finite Element
FEA:	Finite Element Analysis
Fn:	Applied Load
HTC:	Hertz Contact Theory
LRT:	Light Rail Transit

m and n:	Hertz Coefficient
P:	Contact Pressure
Po:	Maximum Contact Pressure
RCF:	Rolling Contact Fatigue
$R_{1w:}$	Wheel Contact Curvature
R_{2w}:	Wheel Radius
$R_{1r:}$	Rail Radius
$R_{2r:}$	Rail Contact Curvature
Sh:	Wheel Flange Height
Sd:	Wheel Flange Thickness
UIC:	International Union of Railway
V:	Operating Speed
$\boldsymbol{\nu}$:	Poisson's Coefficient
$\boldsymbol{\nu}_{w:}$	Wheel Material Poisson's Ratio
$\boldsymbol{\nu}_{r:}$	Rail Material Poisson's Ratio
$\sigma_{1:}$	The principal direct stresses acting along the x axes
$\sigma_{2:}$	The principal direct stresses acting along the y axes
$\sigma 3_{:}$	The principal direct stresses acting along the z axes
$\delta_{w:}$	Parameter Related to Wheel Material
$\delta_{r:}$	Parameter Related to Rail Material
$\boldsymbol{\omega}$:	Angular Velocity

CHAPTER ONE

INTRODUCTION

1.1. Backgrounds

Railways use low resistance of movement between wheel and rail, in order to be an energy efficient mode of transport. The development of fast or heavy trains affects the vehicle-track dynamic interaction. Vehicle-track interaction includes ride comfort and safety, vehicle stability, wheel-rail forces, wheel-rail corrugation, wheel out of- roundness, noise propagation, etc., and is influenced by a variety of factors. Safety is the most important attribute of quality of service and operation for railways. The condition of wheels and rails has a great impact on railway safety.

The interaction in the contact zone between wheel and rail is determined by the global dynamic behavior of the vehicle and by various physical phenomena that occur in the contact zone. The profiles of wheel treads and railheads are transformed by the wheel and rail interaction.

Wheel/rail wear is continuing to be a very important factor limiting asset life. [1] The dynamic behavior of railway vehicles on the track is greatly influenced by wheel-rail interaction. In depth understanding of wheel-rail contact theory enables railway researchers study problems such as wear, rolling contact fatigue, corrugation, friction and track irregularities. [2]

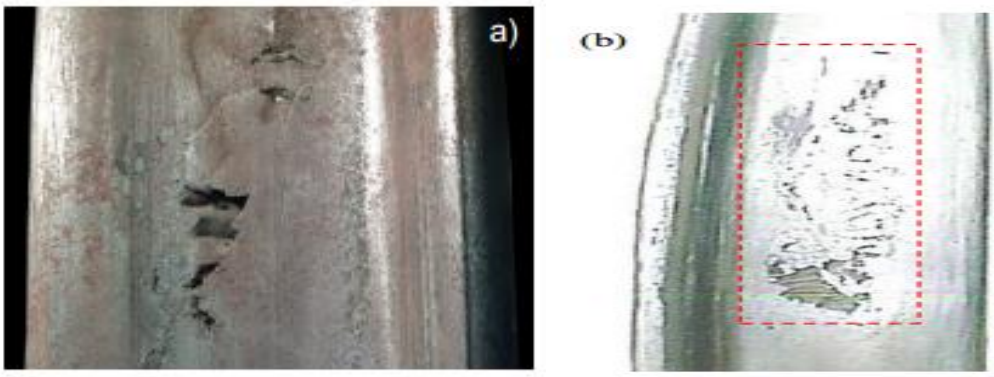

a) Crack in the wheel tread, b) a severe wheel flat with spalling

Figure 1. 1 Wheel damage [9]

The damage assessment in wheel–rail contact is a very complex problem, as is affected by many parameters (materials, load history, climatic conditions and other) and different damage mechanisms can occur. Wear, cyclic plasticity, surface origin rolling contact fatigue (RCF) and sub-surface origin RCF are the key damage mechanisms occurring on wheels and rails that can interact and influence each other. [3]

Damage mechanisms such as surface cracks, plastic deformation and wear can significantly reduce the service life of railway track and rolling stock. They also have a negative impact on the rolling noise as well as on the riding comfort. Higher train speeds and increased axle loads implies that the consequences of larger contact forces between wheel and rail must be thoroughly investigated. [3]

Figure 1. 2 a wheel flat formed by wheel-rail slip in the contact [22]

1.1.1. Rolling Stock Wheel

Wheels and axles are the most critical parts of the railway rolling stock. Mechanical failure of design dimensions can cause derailment. Wheels are classified into solid, tyre, and assembly types. Solid wheels have three major elements: the tyre, the disc, and the hub, and mainly differ in the shape of the disc. Tired wheels have a tire fitted to the wheel disc that can be removed and replaced when it reaches its maximum turning limit. Wheels may have straight, conical, and S-

shaped, spoked, or corrugated type discs when viewed in cross-section. A straight disc reduces the weight of the construction and can be shaped such that the metal thickness corresponds to the level of local stress. The conical and S-shape discs serve to increase the flexibility of the wheel, therefore reducing the interaction forces between the wheels and the rails. Corrugated discs have better resistance to lateral bending. The desire of reducing wheel-rail interaction forces by reducing the unsprang mass has led to development of resilient wheels that incorporate a layer of material with low elasticity modulus (rubber, polyurethane). These help to attenuate the higher frequency forces acting at the wheel-rail interface. Improved bearing reliability aroused interest in independently rotating wheels which provide significant reductions in unsprung mass due to the elimination of the axle. By decoupling the wheels, the independently rotating wheelset inevitably eliminates the majority of wheelset guidance forces. Such wheelsets have found application either on variable gauge rolling stock providing fast transition from one gauge width to another or on urban rail transport where low floor level is necessary.

1.1.2. Rolling stock wheel terminologies / parts

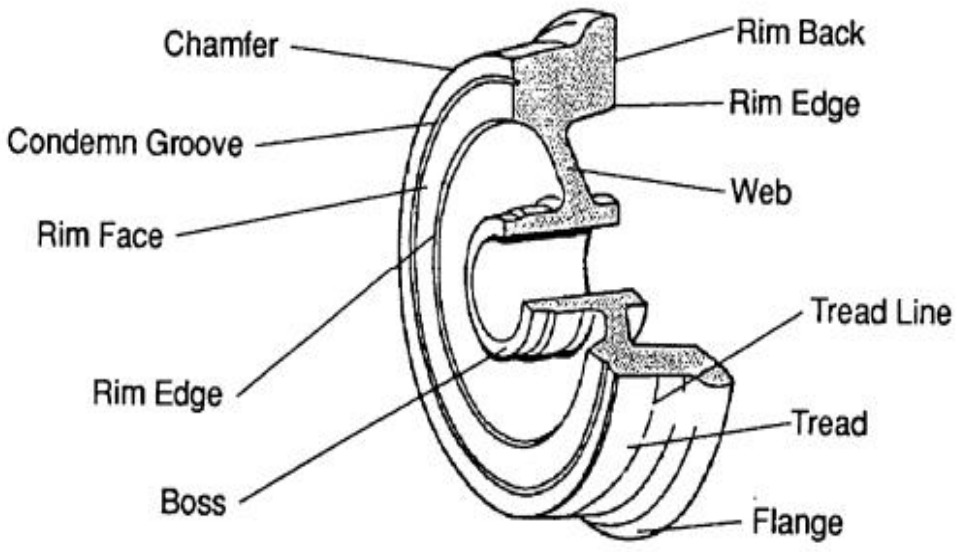

Figure 1. 3 wheel parts

1. Wheel tread: - the outer circumference of the rim, which contacts the rail.

2. Wheel flange: - guidance of the wheelset on the rails.

3. Wheel rim: - running surface, rail-wheel contact.

4. Web: - joins the two parts (hub and rim).

5. Wheel hub: - axle-wheel interference fit assembly.

6. Wheel center: - flexible hub-rim connection.

1.1.3. Wheel Profile

Wheel/rail contact physically occupies an area the size of a small coin, and such contact transfers the load from a vehicle ranging from 3.5 t (28 t lightweight passenger coach) to 17.5 t (heavy freight car of 140 t) per wheel. The material in and around the contact area is therefore highly stressed. High rates of wear might be expected from such contact but, because the load is applied and removed many times during the passage of each train, there is the added possibility of fatigue of the rail surface. The selection of railway wheel and rail profiles is a challenge that has faced engineers since the dawn of the railway age. From the first cylindrical wheels running on flat plates, wheels were made conical to produce better guidance, and flanges were added for safety. Modern wheels often have complex profiles based on the shape of worn wheels in an attempt to increase their life. [4]

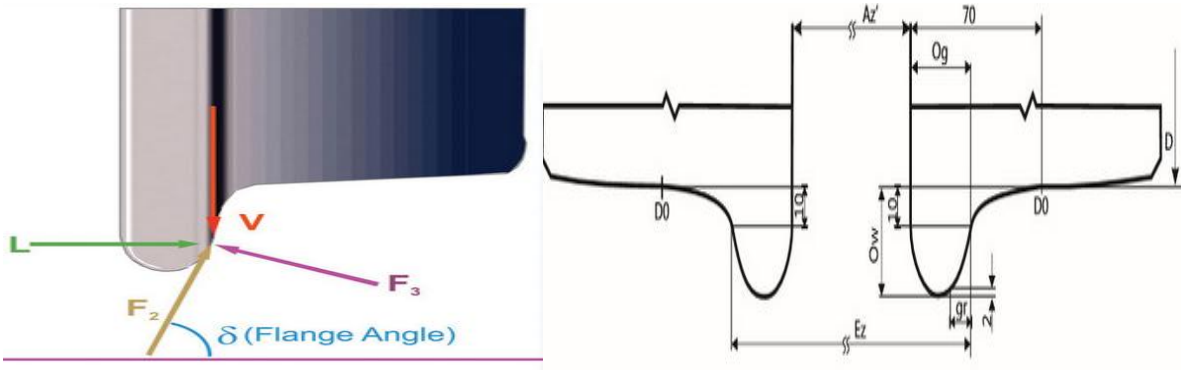

Figure 1. 4 wheel profile

1.1.4. Wheel Wear

Wear is a process of removal of material from one or both of two solid surfaces in solid state contact, occurring when these two solid surfaces are in sliding or rolling motion together. Wear is the progressive loss of materials from contacting surfaces relative in motion. Along with fatigue and corrosion, wear has been known as one of the three major factors limiting the life and performance of an engineering component and an engineering system, whether the system is as big as a heavy machine, or as small as a tiny electronic device.

Damages of wear are twofold. Firstly, the loss of materials from the contacting surface reduces the dimension of the component. This often leads to the increased clearance between the moving parts, and consequently results in high vibration, high noise, reduced efficiency and system malfunction. If dynamic loading is involved, the reduced component dimension could promote fatigue fracture, leading to a catastrophic failure.

Secondly**,** the material detached from worn surface, known as wear debris, is similarly harmful. It may cause contamination, for example, when a machine for food or beverage processing has problems with wear. It may act as abrasive when trapped inside the contacting surface, causing further increased wear rate. The cost of wear is enormous, and thus great efforts have been made ever since the early ages of industry, with aims to reduce or eliminate wear. [5]

In this thesis paper the influence of Overloading on wheel surface damage in the case of AALRT is analyze. To achieve the objectives different assumptions are considered. From this the analysis part will do by using Hertz wheel rail contact theory assumptions and factors which have influences on wheel damage like temperature, environmental conditions and so on are not considered but the effect of loading will analyze by considering different wheel radiuses. The analyses will do using numerical analysis method and ANSYS. Finally after analyses and getting different results, other better wheel material which can resist the current AALRT's loading will be selected.

1.2. Problem Statement

Damages on wheel rail contact are a very complex problem. Wheel rail contacts are affected by many parameters like materials used, loads which are applied, and the wheel rail contact thermal conditions and so on. These parameters (materials, thermal conditions, load…) lead the wheel into different damages like RCF and wear which are the major damage mechanisms on wheel and it decreases the vehicle performances. [3] Now a day AALRT faces a problem on the wheel and it leads the vehicles out of service. These problems on the wheel are because of one of the above mentioned factors. So, it is better to do a research on influence of train overloading (the load which is above the maximum permissible load) on wheel surface damage to select a better material for the wheel to resist the current AALRT loading conditions. In the current situation AALRT give services more than its maximum permissible loading conditions.

1.3. Objectives

1.3.1. General Objective

- Analyze the Influence of Train Overloading on Wheel Surface Damage and selecting better wheel material for AALRT.

1.3.2. Specific Objectives

- .To analyzes wheel/rail contact patches; a (forward) and b (lateral) in AALRT.
- Analyze the applied load (stress) on the contact area (wheel/rail).
- Analyze the effect of overloading on wheel/ rail contacts (AALRT).
- Select better wheel material for AALRT to resist the current loading conditions.

1.4. Significance of the Research

The main focus area of this paper is Analyzing the Influence of Train Overloading on Wheel Surface Damage and selecting better wheel material for AALRT. To achieve the aim of the research contact patch, stress, fatigue life, fatigue damage… will analyzed using ANSYS

software. So this study will be significant for further study of Addis Ababa LRT to know the causes of the damage on the wheel and select a good material for the wheel. By doing so they can increase the life time of the wheel, minimizes delaines to passengers' transportation, provide improved performances and minimizes load sensitivity.

1.5. Scope and Limitations of the research

As stated on problem statement the wheel rail contact is influenced by many parameters like material used, applied load, environmental conditions and so on. But in this research only the influence of applied load on the wheel surface damage is analyzed to select a better material for the wheel to withstand the maximum stress on the contact area.

1.5.1. Scope of the research

The scope of this thesis is analyzing and selecting better wheel material for AALRT to minimize wheel Surface Damage and load sensitivity due to Train overloading (the load which is above the maximum permissible load) in the case of AALRT. The analysis will consider only the contact between wheel and rail on straight track. This thesis will do using CATIA for modeling and analyze by using ANSYS software which are helpful to analyze stress, deformation, fatigue life and fatigue damage at the contact point on different wheel materials.

1.5.2. Limitations of the Research

The limitations of this research are lack of relevant data and references; because of this it is difficult to compare most countries wheel material standards. And need for high performance computer for the ANSYS analysis. And also in this paper materials yield strength and analyzed stress are not compared.

1.6. General Research Methodologies

The research methods are for analyze the influence of overloading on wheel damage in AALRT. In this research paper load and wheel material are considered to be the main causes of the

changes of the wheel profile. Software which is CATIA and ANSYS are considered to be an appropriate tool for modeling and analysis.

- Collecting different data from ERC, different websites and others.
- Analytical analysis of wheel/rail contact.
- Modeling wheel and rail contact assembly using CATIA software.
- Wheel/rail contact Analysis using ANSYS software.
- Wheel materials (stress, deformation, fatigue life) analysis
- Conclusion and Recommendation

Collecting different data's

Collecting and using different data's which are useful for analyzing the contact stresses and shows the impact of overloading from different sources (ERC, journals, articles, researches and interview with some individuals).

Analytical analysis of wheel/rail contact

Analyze analytically the collected data's considering different applied loads on the wheel including overloading which is beyond permissible load.

Modeling wheel and rail contact assembly using CATIA software

Model the wheel and rail using data's which are collected from ERC and assemble the parts of wheel and rail using appropriate dimensions by CATIA.

Wheel/rail contact Analysis using ANSYS software

Analyze wheel rail contact patches and stresses which are modeled and assembled by CATIA and use apply loads on the wheel Centre by using ANSYS. The same structural size and different Mechanical properties are used for different wheel materials.

Wheel materials (stress, deformation, fatigue life) analysis

Analyze the effect of loading on different material of wheel and observe the results (stress, deformation, and fatigue life, damage) to select better wheel material for AALRT to withstand the applied loads.

Conclusion and Recommendation

Evaluation of generated data depends on the numerical and software analysis on acceptable and unacceptable overload results. Using the final observed results of the wheel materials will compared and gives brief discussions on this. This step helps to conclude the effect of overloading and wheel materials damage. And finally Recommendation for Ethiopian Railway Corporation will be provided based on the results of the analysis.

1.7. Organization of the Thesis

The thesis report contains 5 chapters and a brief summary of the chapters is given below:

Chapter 1 Introduction: this chapter describes the general introduction about wheel rail contact, Rolling Stock Wheel, Wheel Wear, statement of the problem, objective, scope and limitations.

Chapter 2 Literature Review: this chapter reviews published research relevant to the thesis topic. Wheel/Rail Contact, Mechanism of Wheel/Rail Contact, Wear Mechanism, are presented.

Chapter 3 Numerical Analysis: this chapter describes the analytical contact solutions of wheel rail contacts. Such as contact patch, contact pressure, and principal stresses.

Chapter 4 Result and Discussions: In this chapter result of the analysis and discussion of the analysis results will present.

Chapter 5 Conclusion and Recommendation: this chapter presents the final conclusions, recommendations and future work of the thesis.

CHAPTER TWO

LITERATURE REVIEW

2.1. Wheel/Rail Contact

Steel wheels rolling on steel rails are the principal characteristic that distinguishes railways from other forms of transport. Wheel and rail meet at a contact patch that is small and carries the full wheel load through which all steering, traction, and braking forces are transmitted. This contact patch sees a severe working environment. Stresses normal to the plane of contact can reach values several times the wheel or rail tensile strength, and sometimes shear stresses in the plane of contact can exceed the shear yield stress. Rapid temperature rises, caused by relative slip between the wheel and rail, can reach several hundred degrees Celsius in routine operation, and over 1000°C in extreme circumstances. These stress and temperature conditions inevitably lead to wear, deformation, and damage to the wheels and rails; and a major goal of railroads is to arrange service conditions and maintenance procedures to minimize deterioration and hence extend component life. This is important because rails and to a lesser extent wheels constitute a large part of a railroad's asset base. Extending the life of these components, and especially that of the rail, has a major impact on railroad profitability. An understanding of the tribology of the wheel/rail system is essential if wheel/rail life is to be extended. This system is complex, and its behavior depends on interactions between the materials (wheel, rail, and any third body introduced, such as lubricant/debris mixtures) and the stress-temperature environment (among other things, a function of vehicle weight, vehicle/track interaction, wheel/rail profiles, wheel/rail adhesion, and speed). [1]

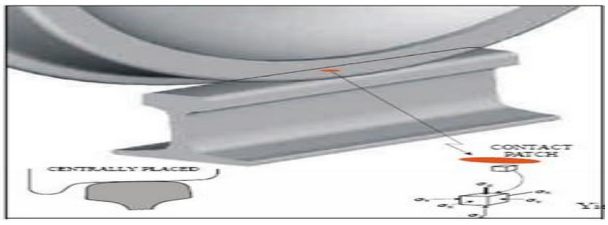

Figure 2. 1 Contact between wheel and rail

When two bodies (wheel and rail) are in contact, stresses and strains appear. A large force from the first body (wheel) is transferred to the second body (rail) through a small contact region about 1cm to 2cm. [6]

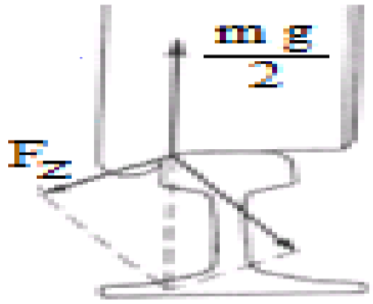

Figure 2. 2 Rolling contact forces [6]

a) Region A - wheel tread rail head contact:
   - most common contact region;
   - Lower contact stress.

b) Region B – wheel flange rail gauge corner:
   - much smaller contact area and more severe;
   - Higher contact stresses and wears rates.

c) Region C - wheel and rail field sides contact:
   - least likely contact region;
   - Higher contact stress.
   - Undesirable wear, lead to incorrect steering of wheel set.

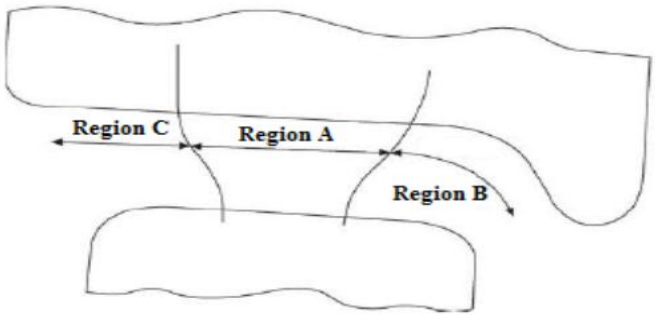

Figure 2. 3 Wheel rail contact zones [6]

2.2. Mechanism of Wheel/Rail Contact

Rail/wheel interaction is essentially a tribological problem involving rolling and sliding contact. Therefore, the geometry of contact of the wheels on the rail and the resulting surface and sub-surface stresses need to be understood in order to assess the mechanisms of surface damage and rail failure. Studies to date show that the main concerns are a combination of rolling contact fatigue and wear. Which of these dominates will depend upon the properties of the rail steel, lubrication, contact load, train speed, traction, rail radius of curvature and defects on rail and/or wheel. Changes in the wheel-rail profile due to degradation a process increases rail-wheel contact forces and ultimately leads to higher damage propagation. [7]

Dynamic loading arises from the progression of the train along the track and from traction, braking and steering forces, and the contact is more precisely described by a multipoint contact pressure distribution than a Hertzian one. Hertz's method assumes that contact surfaces are smooth and can be described by a second degree polynomial. It also assumes that there is no friction force between the contacting surfaces and that the contact stress field is in a semi-infinite half space. Hertz's method gives an elliptical contact patch with semi axes that can be calculated. Kalker's theory takes into account the evolution of adhesion (adhesion parameters T/N) as a function of sliding, which takes place in three stages: (a) a linear pseudo-sliding phase, (b) a nonlinear pseudo-sliding phase and (c) a complete sliding phase. The contact stresses between rail and wheel die away approximately three contact widths from the area of translational contact between wheel and rail. The tangential stresses can be divided into two parts. One is parallel to the direction of wheel rotation and the other is perpendicular to the direction of wheel rotation. High tangential stresses arise from dynamic loading (traction, braking and steering forces). In each case, for low rail, the contact stresses are almost identical. High rails are used where the traffic is dense, high axle loads and high speed trains are used in which head height is higher than the normal. This will allow grinding the head of the rail to remove surface defects, instead of replacing rails for minor surface defects. [7]

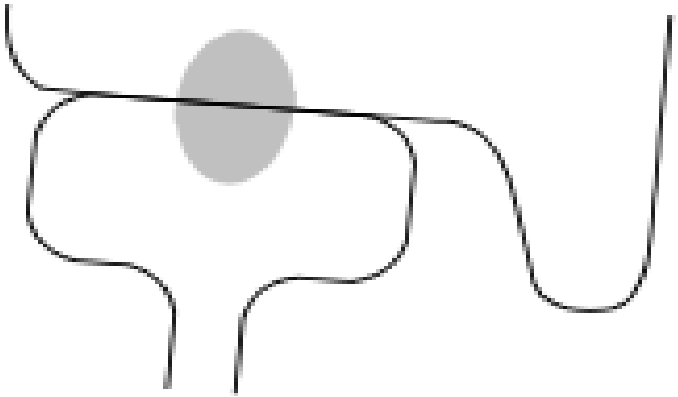

Figure 2. 4 Wheel tread and rail head contact

Telliskivi and Olofsson have analysed the rail-wheel contact problem using Finite Element Analysis (FEA) applied to actual measured rail-wheel profiles comparing their results with Hertz's analytical method and Kalker's approach. [7] The use of FEA allows the assumptions of the Hertz model to be transcended and allows creep, wheel spin and associated forces to be taken into account as well as plastic deformation and the existence of non-metallic inclusions in the steel. Rail and wheel contacts near the gauge corner and on the rail head were analyzed using FE and compared with analytical methods. The analytical contact pressures were higher than FE analysis when rail-wheel contact was at a gauge corner probably due to the half space assumption and material model, while, during rail-wheel contact on the rail head (when the radii of curvature of the two contact bodies at the contact point are large compared with the dimensions of the contact area).

Iwnicki has summarized the contact forces acting during train running on straight and curved track. [8] Obviously, all contact forces arise at the rail/wheel contact and the contact area depends critically on the detailed relative wheel and rail geometries. Contact patch forces can be split into normal and tangential components, and the tangential force split further into a longitudinal force, which is parallel to the direction of train travel, and a lateral force, which is perpendicular to the direction of wheel travel. The normal (vertical) force is caused by axle load and the lateral force arises because of the irregularities and curvature of the track. Lateral forces are also associated with accelerations, either due to picking up speed or braking and/or changes in direction around curves. These lateral forces are transmitted to the rail at the contact patch, and are associated with creep forces which initiate from micro-slippage in the area of contact.

Larger creep is possible if the wheel flange rubs on the track. Flange rubbing on the rail causes higher shear stress and consequently micro slip (creep) before sliding when the shear strength is exceeded. This is the source of the highest stress produced by any part of the wheel tread rolling on the rail.

2.3. Materials used for Wheels on Rolling Stock

The materials employed in wheels and rails in Europe are steels whose predominantly pearlite structures containing hard cementite having high resistance to wear. According to UIC Leaflet 812-3 for solid wheels lists seven types of steel, which mainly differ in carbon content, heat treatment state and therefore strength, and EN 13262 contains only four types. Grade R1 for freight wagon wheels is becoming less favorable than the standard R7 material, and Grades R2/R3 has never been used in operational practice. R7 is the most commonly used grade. It is used for all freight wagon wheels and on most passenger vehicles. Where wheels made from R7 are intended for use in vehicles with tread brakes. Experience has shown that where carbon content exceeds 0.5%, the KIC values of 80MPa √m can only be attained where comparatively small grain size (fine grain), high purity and high homogeneity are present in the microstructure throughout the circumference of the wheel. This places heavy demands on manufacturing quality. For this reason, these wheels are commonly supplied with lower carbon contents (<0.5%C) which puts them often in the lower strength tolerance range, so that besides pearlite, large amounts of pre-eutectoid ferrite are present in the tread. Although this leads to greater toughness, the wear resistance is correspondingly diminished. According to Deutsche Bahn's (DB) experience, a free (pre-eutectoid) ferrite content of ≤10% is advantageous in terms of minimizing wheel wear at the tread. For driven wheels on locomotives and motor coaches, R8 is increasingly the used grade. In summary, materials employed for solid wheels in Europe are largely restricted to unalloyed steels with maximum carbon content of 0.56% and – after appropriate heat treatment (fine pearlitization) of the tread – tensile strengths of at least 820 to 980MPa in maximum [9].

Table 2. 1 wheel steel requirements according to UIC 812-3 and EN 13262 [9]

Steel category		Carbon content	Yield strength (MPa)	Tensile strength (MPa)	Elongation (%)
UIC 812-3	EN13262	UIC/EN	EN13262	UIC/EN	UIC/EN
R1N	-	≤ 0.48	-	600-720	≥ 18
R2N	-	≤ 0.58	-	700-840	≥ 14
R3N	-	≤ 0.70	-	800-940	≥ 10
R6T,E	ER6	≤ 0.48	≥ 500	780-900	≥ 15
R7T,E	ER7	≤0.52	≥ 520	820-940	≥ 14
R8T,E	ER8	≤ 0.56	≥ 540	860-980	≥ 13
R9T,E	ER9	≤ 0.60	≥ 580	900-1050	≥ 12

Wheel grade applications

Table 2. 2 Recommended grades per railway network

Applications	Wheel load	USA (AAR)	UK(BS)	Europe (EN)	China (TB/T)
Locomotives	Heavy	C or B	R8T	ER8	CL60
Passenger	*Light*	*L*	*R8T*	*ER6 or ER7*	*CL60*
Passenger	Moderate	A	R8T	ER6 or ER7	CL60
Passenger	Heavy	B	R8T	ER6 or ER7	CL60
Passenger	Heavy	C	R8T	ER6 or ER7	CL60

In the case of Ethiopia, AALRT uses CL60 wheels for passenger services and U74 rails.

2.4. Wear Mechanism

Wear is the loss or displacement of material from a contacting surface. Material loss may be in the form of debris. Material displacement may occur by transfer of material from one surface to another by adhesion or by local plastic deformation. There are many different wear mechanisms that can occur between contacting bodies, each of them producing different wear rates. The simplest classification of the different types of wear that produce different wear rates is "mild wear" and "severe wear". Mild wear results in a smooth surface that often is smoother than the original surface. On the other hand, severe wear results in a rough surface that often is rougher than the original surface. Mild wear is a form of wear characterized by the removal of materials in very small fragments. Mild wear is favorable in many cases for the wear life of the contact as it causes a smooth run-in of the contacting surfaces. However, in some cases it has been observed that it worsens the contact condition and the mild wear can change the form of the contacting surfaces in an unfavorable way. Another wear process that results in a smooth surface is the oxidative wear process characterized by the removal of the oxide layer on the contacting surfaces. In this case the contact temperature and asperity level influence the wear rate. Abrasive wear caused by hard particles between the contacting surfaces can also cause significant wear and reduce the life of the contacting bodies. [10]

In wheel–rail contact, both rolling and sliding occur in the contacting zone. There can be a large sliding component on the contact patch at the track side of the rail head (gauge corner). Due to this sliding, wear occurs in the contact under the poorly lubricated condition that is typical of wheel–rail contact. An observation that can be made on sliding wear is that an increase of the severity of loading (normal load, sliding velocity, or bulk temperature) leads, at some stage, to a sudden change in the wear rate (volume loss per sliding distance). The severe wear form is often associated with seizure. The transfer from mild acceptable wear to severe/catastrophic wear depends strongly on the surface topography.

The loading capability of a sliding contact may be increased considerably by smoothing the surface. Chemo reacted boundary layers imposed by additives in the lubricant can improve the properties of lubricated contacting surfaces and reduce the risk of seizure. Also, as shown by

Lewis and Dwyer-Joyce, the surface temperature influences the transition from mild to severe wear. In addition to the contact pressure and the size of the sliding component, natural and applied lubrication strongly influenced the wear rate for the full-scale. The curve radius of the track has a strong influence on rail wear. The influence also strongly depends on the vehicles and their behavior. [10]

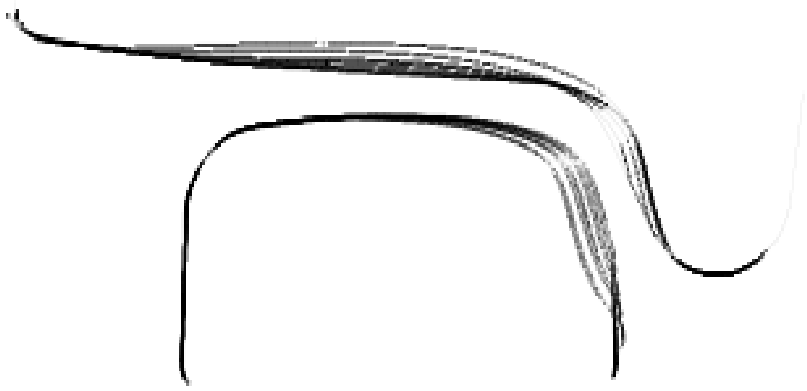

Figure 2. 5 Change of wheel and rail [15]

Fikru Bekele (2014) has work on the effect of change of wheel-rail contact geometry on contact fatigue stresses. In his work he discussed on the results, Effect of change of wheel taper angle (conicity) on fatigue parameters, Effect of change of radius of curvature of wheel on fatigue parameters, Effect of change of radius of curvature of rail on fatigue parameters, and concludes that the use of small conicity decreases both rolling contact fatigue phenomenon and wheel wear. [11]

Ayana Gebremichael (2014), Analysis of Rolling Contact Fatigue Damage and Fatigue Life Comparison of Rail Due to Cyclic Axle Load. The purpose of this paper is analysis of rolling contact fatigue and show the fatigue life of wheel/rail due to the cyclic axle load applied. Also the fatigue life comparison of the rail between ANSYS software and experimental test on the samples prepare from the rail. In his paper he conclude that as far as fatigue life of rail is concerned, the suitable cyclic axle load and proper maintenance before crack initiate and propagate may be regarded as the best possible life improvement operation. [12]

Paul Molyneux-Berry, Claire Davis and Adam Bevan (2014) do a research on the Influence of Wheel/Rail Contact Conditions on the Microstructure and Hardness of Railway Wheels in the objectives of investigate the influence of the as-manufactured steel microstructure and hardness along with the influence of wheel/rail contact conditions on the observed damage (such as rolling contact fatigue (RCF) cracks and plastic flow) on the tread of railway wheels. And they conclude that measured hardness through the depth of an "in-service" wheel rim varies significantly, with three distinct effects. The underlying hardness trend (hardness decrease with depth below the tread, excluding contact stress effects), The near-surface layer (generally less than 1mm deep) exhibits plastic flow and micro structural shear as a consequence of wheel/rail contact forces which can considerably exceed the yield stress of the undeformed material and In a layer approximately 1mm–7mm deep, the wheel/rail contacts cause stresses in excess of the (undeformed) material yield stress, leading to work hardening. [13]

Sergey M. Zakharov (2002) did a research on simulation of mutual wheel/rail wear. The author take a suggested approach assumptions which are for particular conditions, the steady-state profile exists and depends on the initial wheel/rail profiles and on tribological properties of materials; there exists an optimal, upon selected criteria, profile providing the minimum wear rate or the minimum pressure distribution; the optimal profiles are selected for a family of wheel flange/rail head conformal profiles; to find optimal profiles the condition of the constant ratio of wear rate of contacting bodies at the contact area is set; the vertical and the lateral forces, as well as the angle of wheel to rail attack are known from calculation of the quasi-static movement of a bogie in a curve; the dependence of the wear rate from the contact parameters is derived from the laboratory simulation of wheel flange/rail head wear. And concludes the theoretical study of two mutually wearing bodies has shown that their steady-state worn profile depend on their initial profiles. [1]

Tanel Telliskivi, Ulf Sellegren and Ulf Olofsson: A tool and a method for FE analysis of wheel and rail interaction. A tool for contact mechanics modeling and simulation of the wheel rail contact has been developed. The geometry of the contact can easily be changed. The model can

be generated from measured wheel and rail profiles. Traditional methods and computational tools are limited by a half space assumption and a linear material model. [3]

Arthur Anyakwo, Crinela Pislaru and Andrew Ball (2012); A New Method for Modeling and Simulation of the Dynamic Behavior of the Wheel-rail contact and finally they riches to a conclusion of wheel-rail geometry and efficient solutions for normal and tangential contact problems representing the wheelset dynamic behavior on the track. The lateral displacement of the wheelset and the yaw angle are taken into account. [2]

Research Gap

From reviewed different literatures, wheel rail contact stresses and damages are analyzed. But most researchers are focused on rail surface damage in wheel rail contact due to cyclic loading, temperature and so on and also they did not recommended other materials which can resist the problem. But in this research wheel damage due to Overloading (loads beyond its maximum permissible load) on wheel rail contact in the case of Addis Ababa LRT will be analyze and other materials will select which can resist the problem (current loading conditions).

CHAPTER THREE

NUMERICAL ANALYSIS

Wheel set is the most important component among the different components of a car and this component plays a very important role in safety and also economic issues for the railway industry.

From safety point of view, wheel profile should be able to ensure the consistent movement of car movement, and from economic point of view, this issue should be kept in mind that a lot of financial sources are spent annually to replace or turn a wheel in the railway transportation system.

The trend towards increasing the speed of trains on rail tracks and the increase of axle load has resulted in higher wheel-rail contact forces. Such forces are the main causes of wheel damages including wear and fatigue.

3.1. Material properties

Table 3. 1 Chemical Composition [23], [24]

	C%	Si%	Ma%	Po%	S%	Cr%	Co%	Mb%	Ni%
CL60	0.55	0.17	0.50	0.040	0.040	0.25	0.25	N/S	0.25
ER7	0.52	0.40	0.80	0.020	0.015	0.30	0.30	0.08	0.30
R8T	0.56	0.40	0.80	0.020	0.015	0.30	0.30	0.08	0.30

Table 3. 2 Mechanical Properties [9]

	Tensile strength	Yield strength	Elastic modules	Poisson's ratio
CL60	910MPa		210GPa	0.3
ER7	940MPa	520MPa	206GPa	0.27
R8T	980MPa	540MPa	206GPa	0.285

3.2. Contact Types

3.2.1. Conformal

- Conformal: the two bodies fit closely together without deformation
- The contact area is larger
- In wheel-rail application the two bodies could have a conformal contact if they both have similar profile at the contact area (eg. contact between the gauge corner of the rail with the wheel throat)

Figure 3. 1 Conformal contact (between the gauge corners of the rail with the wheel throat) [4]

3.2.2. Non-conformal contacts

- Non-conformal: contact between two dissimilar profiles
- The contact is a point/a line contact without deformation
- The contact area is generally small compared to the dimension of the bodies in contact
- The stress/deformation is locally at the contact region
- In wheel-rail application the two bodies often have a non-conformal contact (eg. contact between the rail head and wheel tread)

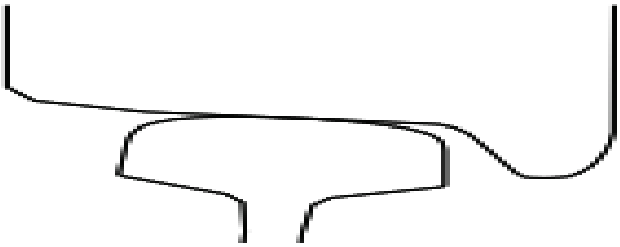

Figure 3. 2 Non-conformal contact (between wheel tread and rail head) [4]

3.3. The Hertzian Contact of Wheel and Rail

Initially the stresses and deformations of static contact, generated from a normal force. For an initial analysis, estimation of contact areas and material deformations are still based upon the theory of Hertz.

These covered the:-

- frictionless,
- elastic,
- Compressive contact of non-conforming solid bodies.

His basic formulas are still used for rapid determinations of:-

- contact stress,
- area and deformation in engineering contacts including wheel-rail

3.3.1. Hertzian theory assumptions

- The surfaces are frictionless;
- The surfaces are continues and non-conformal;
- The contact area is very small compared with the bulk volume of the two bodies;
- The contact stresses are large compared with other stresses in the two bodies.

Wheel/rail contact can be represented by a conical surface (the wheel) on a hemi-spherical cylindrical surface (the rail head) as shown in the figure. The area of such a contact is elliptical.

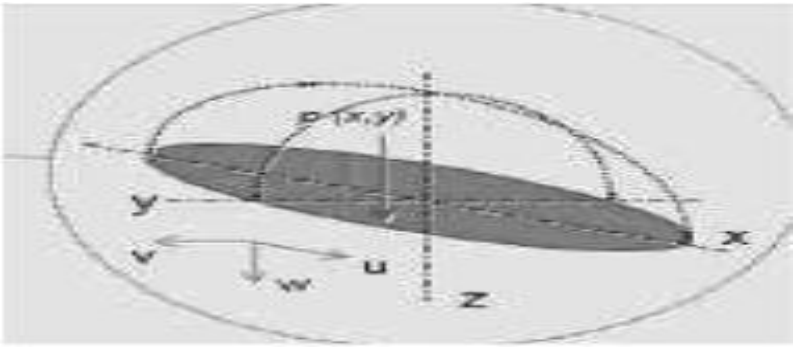

Figure 3. 3 Elliptical of the contact area between wheel and rail [14]

3.4. Basic wheel parameters of AALRT

Wheel diameter:

- ✓ 660mm (new)
- ✓ 580mm (wear to limit)

Height of wheel flange (Sh):

- ✓ 28mm (new)
- ✓ 25mm (during operation period / only for consulting, this value will be define by the experience of the user)

Thickness of wheel flange (Sd):

- ✓ 21.21mm (new)
- ✓ 15mm (during operation period / only for consulting, this value will be define by the experience of the user)

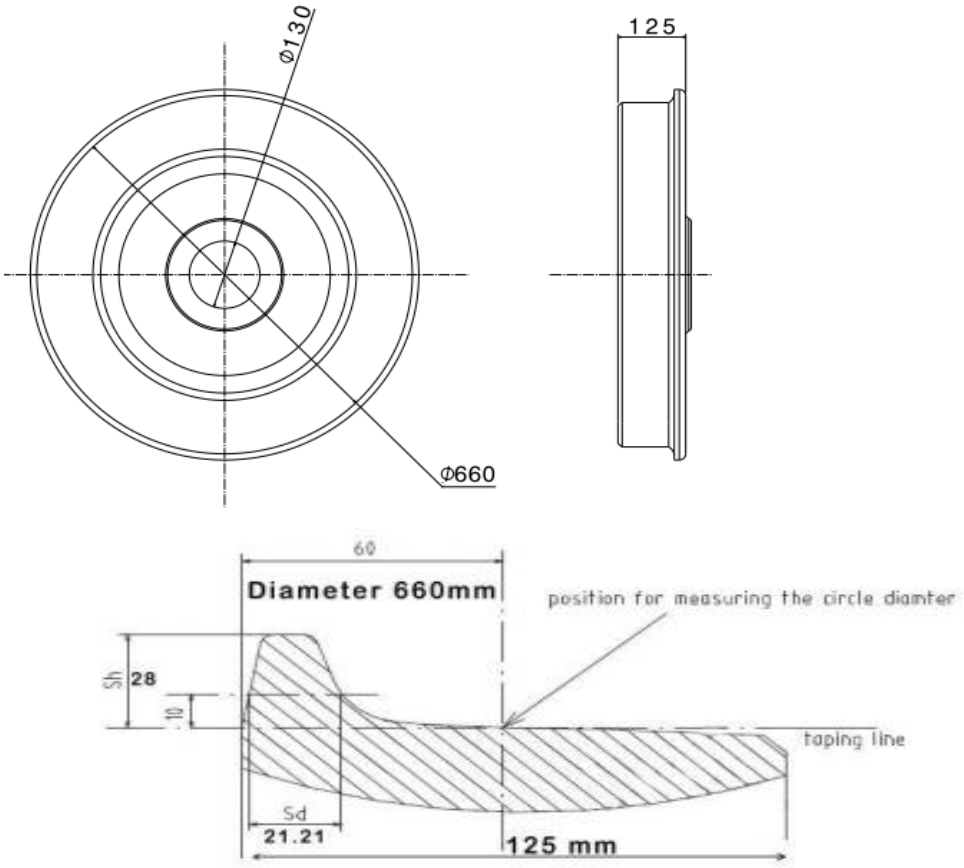

Figure 3. 4 wheel drawing (source: ERC)

3.5. Basic technical parameters of AALRT

Table 3. 3 Basic technical parameters of AALRT

Technical parameter	Parameter value
Track gauge	1435mm
Minimum radius of vertical curve	1000m (auxiliary line)
Minimum radius of horizontal curve	25m
Axle load	≤11(1+3%) t
Maximum gradient	50‰
Rated voltage	DC750V
Train length (w/o train couplers)	28800mm
Maximum width	2650mm
Height	3610mm
Floor level to rail level at low-floor area	380mm (350 at door areas)
Floor level to rail level at high-floor area	655mm
Center to center distance between both bogies	10400mm
Axle distance of the motor unit	1900mm
Axle distance of the trailer unit	1800mm
Clear height in passenger compartment at low – floor area	2255mm
Clear height in passenger compartment at high – floor area	1980mm

Source: ERC (Ethiopian Railway Corporation)

3.5.1. Passenger Capacity

The occupied area of standing passengers is 6 persons/m^2 for rated passenger capacity or 8 persons/m^2 for over-crowed capacity; the average weight of the passenger is 60kg/person.

Table 3. 4 AALRT load capacity

Working condition	Seating capacity	Standing capacity	Total capacity (persons)	Total weight (t)
AW0	0	0	0	About 44
AW2	65	0	65	About 47.9
AW3	65	189	254	About 59.2
AW4	65	252	317	About 63

Source: ERC (Ethiopian Railway Corporation)

3.6. Wheel/Rail Profiles and Theories Governing the Contact Area

Wheel is the means of movement and guiding the car on rail. Wheel diameter in Addis Ababa LRT is between 660 mm which is increased if the axle load is increased. Since the bogie axles are of solid type, and on the other hand, the width of the track is a bit more than the outer distance between two flanges of the wheel, there will be a gap between the wheel flange and side of the rail. Thus, forward movement of the bogie can be accompanied by the lateral movement of axle. Type of wheel profile in AALRT is consistent with Chinese standard CL60. Based on the variety of the capacity of passenger and load transportation (number of compartments and the lay out of the train), their wheel diameters are also different. [14]

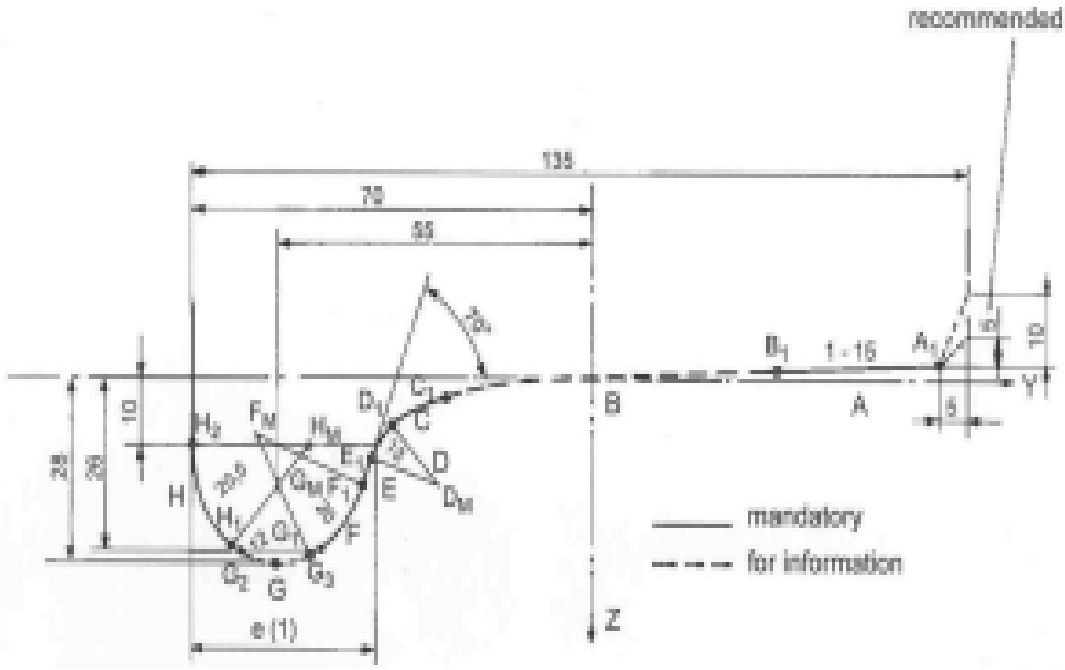

Figure 3. 5 E.g. of Wheel profile of type UIC S1002 [14]

Hertz theory applies the contact area of the tread and the area above the rail. To calculate the contact stresses in the contact area of wheel and rail, geometrical parameters of wheel and rail (major and lateral curve radius), mechanical properties of wheel and rail (elasticity module and Poisson coefficient) should be clarified. Because of wheel profile conisity of wheel profile, wheel movement on rail is accompanied by lateral displacement. So, contact stresses are variable at any given time. Contact stresses in different points on wheel surface are calculated based on Hertz theory.

To calculate the contact stresses in the contact area of wheel and rail, geometrical parameters of wheel and rail (major and lateral curve radius), mechanical properties of wheel and rail (elasticity module and Poisson coefficient) should be clarified.

Table 3. 5 Parameters of (a) wheel and (b) rail

a)

	Mechanical property		**Geometrical parameters**	
Wheel type	Elasticity module (E)	Poisons coefficient($\boldsymbol{\mathcal{V}}$)	Wheel Radius (R_{2w})	Wheel contact curvature (R_{1w})
CL60	210GPa	0.3	330mm	1098mm
ER7	206GPa	0.27	330mm	1098mm
R8T	206GPa	0.285	330mm	1098mm

b)

	Mechanical property		**Geometrical parameters**	
Rail type	Elasticity module (E)	Poisons coefficient($\boldsymbol{\mathcal{V}}$)	Rail Radius (R_{1r})	Rail contact curvature (R_{2r})
50kg/m (U74)	210GPa	0.3	∞	300mm

The theory governing the wheel/rail contact (Hertz theory) describes that when two solid materials are compressed to each other by vertical loads, their contact area is formed. Shape and the value of the contact area between two elastic materials are at static mode.

R_{1w} is considered as wheel contact curvature;

R_{2w} is considered as the major rolling radius of the wheel;

R_{2r} is considered as rail contact curvature; and

R_{1r} as the major rolling radius of the rail (which is normally infinite in rails), as the lateral curve radius of the width of the wheel profile at the contact area and is the lateral curve radius of rail

profile curve. Since the radius of wheel and rail is different from each other, the contact area will be ellipse.

Hertz theory is considered based on material behavior in the contact area, and ignoring friction coefficient.

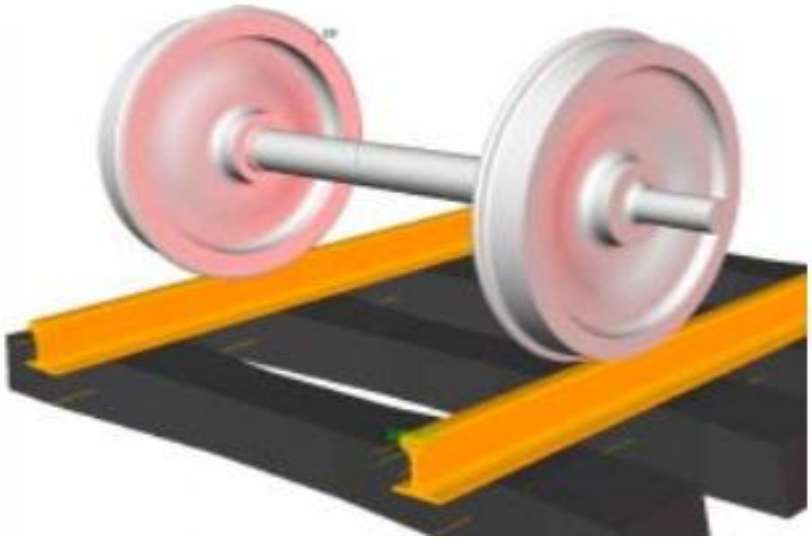

Figure 3. 6 A wheelset on a straight track [3]

If two elastic nonconforming bodies contact together then according to the Hertz contact theory, the contact area is elliptical in shape with a major semi-axis a and a minor semi axis b.

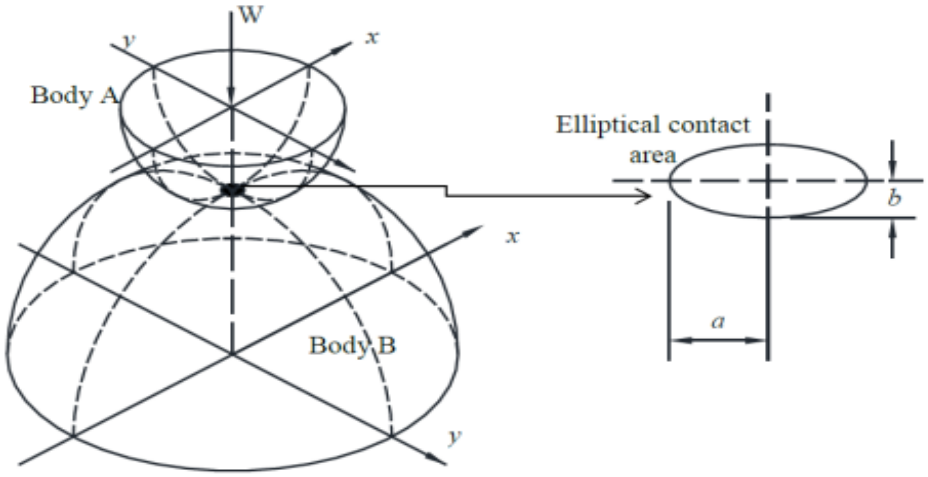

Figure 3. 7 Geometry of two elastic bodies with convex surfaces in contact [15]

3.7. Mathematical Model for Wheel-Rail Contact

Based on Hertz theory claiming that contact area in front of the curve radius of two objects should be minimal, this theory is not applicable whenever there is a wheel flange and rail rim contact. Thus, Hertz theory only applies the contact area of the tread and the area above the rail. To calculate the contact stresses in the contact area of wheel and rail, geometrical parameters of wheel and rail (major and lateral curve radius), mechanical properties of wheel and rail (elasticity module and Poisson coefficient) should be clarified. Because of wheel profile conisity of wheel profile, wheel movement on rail is accompanied by lateral displacement. So, contact stresses are variable at any given time. Contact stresses in different points on wheel surface are calculated based on Hertz theory.

First, According to Hertz [15], if two elastic nonconforming bodies are pressed together then the contact area assumes elliptical shape with a semi major axis ‘a’ and a semi minor axis ‘b’. The distribution of the contact pressure in this elliptical area as shown in the Fig. 3.8 below represents a semi-ellipsoid, expressed as:

$$P = Po\left(1 - \frac{x^2}{a^2} - \frac{y^2}{b^2}\right) \quad \text{.....3.1}$$

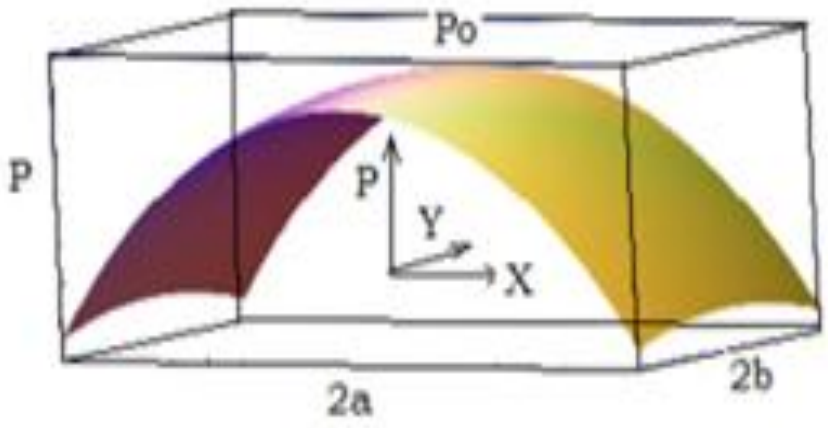

Figure 3. 8 pressure distribution across elliptical area [18]

The method assumes the contact surfaces to be smooth, so they can be described by a second degree polynomial.

$$Z_1 = A_1X^2 + A_2XY + A_3Y^2 \quad \text{.....3.2}$$

$$Z_2 = B_1X^2 + B_2XY + B_3Y^2 \quad \text{.....3.3}$$

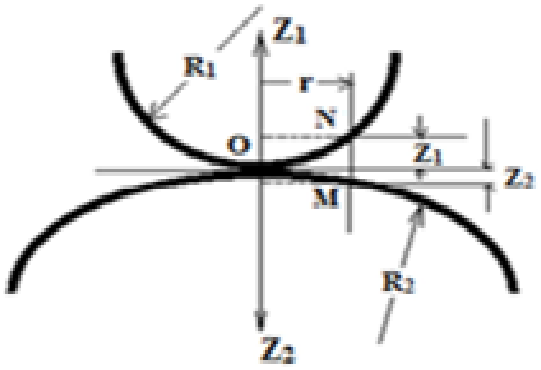

Figure 3. 9 General profiles of two contacting bodies [18]

δ_w and $\delta_{r;}$ are constants given by: $\delta w = \frac{(1-\nu w^2)}{\pi E w}$ and $\delta r = \frac{(1-\nu r^2)}{\pi E r}$, $\boldsymbol{\nu}$ and E are elastic constants.

The distribution of pressure P is found by assuming the intensity of pressure over the surface of contact to be represented by the ordinates of a semi-ellipsoid constructed on the surface of contact [16]. The maximum pressure is obtained occurs at the center of the surface of contact is given by [17]:

$$Po = \frac{3F}{2\pi ab} \quad \text{.....3.4}$$

The semi axes of the elliptic boundary of the surface of contact 'a' and 'b' are given by:

$$\left(\frac{a}{m}\right)^3 = \frac{3\pi Fn(\delta w+\delta r)}{4(A+B)} \quad \text{.....3.5}$$

$$\left(\frac{b}{n}\right)^3 = \frac{3\pi Fn(\delta w+\delta r)}{4(A+B)} \quad \text{.....3.6}$$

The calculation of the contact areas requires knowledge of some geometric constants used in the above formulation. With respect to wheel-rail configuration, the following curvature combinations are related as:

$$2(A+B) = (1/R_{1w} + 1/R_{2w} + 1/R_{1r} + 1/R_{2r}) \quad \text{.....3.7}$$

$$2(B-A) = \sqrt{[(1/R_{1w} + 1/R_{2w})^2 + (1/R_{1r} + 1/R_{2r})^2 + 2(1/R_{1w} - 1/R_{2w})(1/R_{1r} - 1/R_{2r})\cos 180]} \quad \text{.....3.8}$$

Where A and B are positive constants. R_{11} (R_{2w}), R_{12} (R_{1w}), R_{21} (R_{1r}) and R_{22} (R_{2r}) are defined as the principal relative radii of curvature, represented pictorially in the Fig.

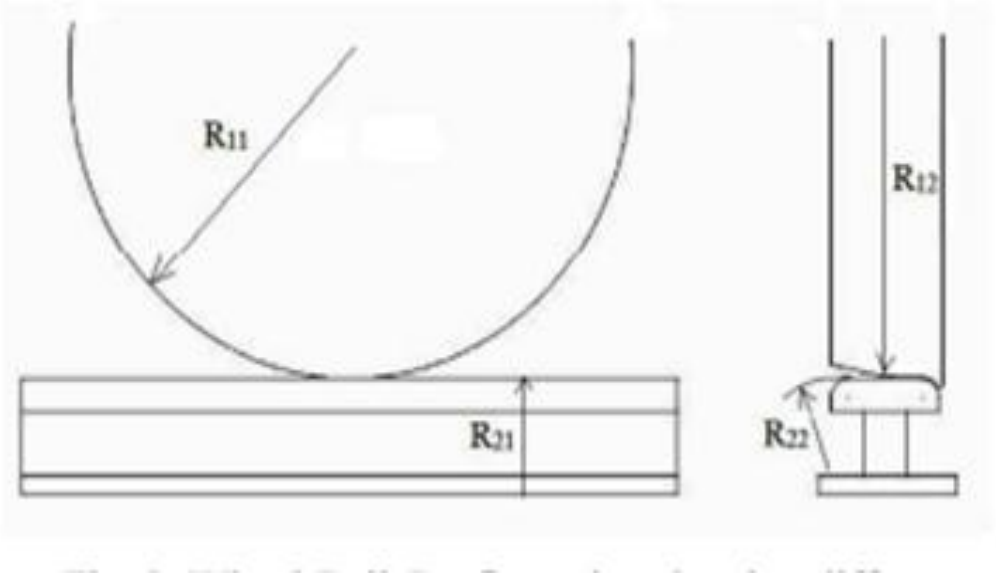

Figure 3. 10 wheel/rail configuration showing d/t principal relative radii of curvature [18]

Where,

R_{11} (R_{1w}): The rolling radius of curvature of the wheel.

R_{12} (R_{2w}): The radius of the wheel profile, which goes to infinity for a conical wheel.

R_{21} (R_{1r}): The radius of the runway which is infinity in this case.

R_{22} (R_{2r}): The radius of curvature of the rail in the plane of cross section.

Therefore;

- R_{1w} is considered as wheel contact curvature = 1098mm
- R_{2w} is considered as the major rolling radius of the wheel = 330mm
- R_{2r} is considered as rail contact curvature = 300mm
- R_{1r} as the major rolling radius of the rail = ∞

After determining and getting different essential parameters of wheel and rail; it is possible to calculate the contact patch at the contact area between wheel and rail.

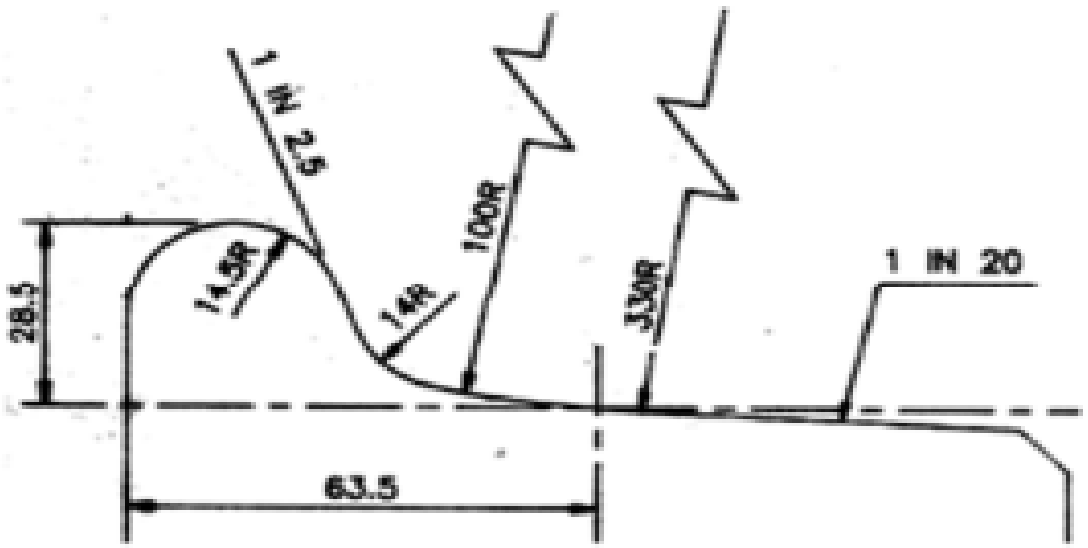

Figure 3. 11 Wheel Profile as China railway standard

δw and δr are the parameters related to the material of the components can be calculated as [18]:

$$\delta w = \frac{(1 - \mathcal{V}w^2)}{\pi E w}$$

$$\delta w = \frac{(1 - 0.3^2)}{\pi * 210 * 10\text{^}9}$$

$\delta w = \underline{1.38*10^{-12}}$

$$\delta r = \frac{(1 - \mathcal{V}r^2)}{\pi E r}$$

$$\delta r = \frac{(1 - 0.3^2)}{\pi * 210 * 10\text{^}9}$$

$\delta r = \underline{1.38*10^{-12}}$

To calculate the elliptical contact area using Hertz theory, the above equations: Eq. (3.7) and Eq. (3.8) are applied;

$2(A+B) = (1/R_{1w} + 1/R_{2w} + 1/R_{1r} + 1/R_{2r})$

$2(A+B) = (1/1098 + 1/330 + 1/\infty + 1/300)$

$A+B = \underline{0.00364}$

$2(B-A) = \sqrt{[(1/R_{1w} + 1/R_{2w})^2 + (1/R_{1r} + 1/R_{2r})^2 + 2(1/R_{1w} - 1/R_{2w})(1/R_{1r} - 1/R_{2r}) Cos180]}$

$2(B-A) = \sqrt{[(1/1098 - 1/330)^2 + (1/\infty - 1/300)^2 + 2(1/1098 - 1/330)(1/\infty - 1/300) Cos180]}$

$B-A = \underline{0.00061}$

After calculating B-A and A+B; now it is easy to find the contact angle β between the wheel and rail. This contact angle β helps to determine hertz coefficient m and n to find the two elliptical contact parameters a and b.

The coefficients m and n are Hertz coefficients and they are given as a function of the angleβ.

$$Cos\beta = \frac{B-A}{A+B} \quad \text{.....3.9}$$

$$Cos\beta = \frac{0.00061}{0.00364}$$

$\underline{\beta = 80.4 = 80 \text{ deg.}}$

By using the Hertz coefficient table and linear interpolation method the value of m and n can be determined.

Table 3. 6 Hertz coefficient m and n [15]

β (deg.)	m	n	β (deg.)	m	n	β (deg.)	m	n
0.5	61.4	0.1018	10	6.6	0.311	60	1.49	0.72
1	36.89	0.1314	20	3.81	0.413	65	1.38	0.76
1.5	27.48	0.1522	30	2.73	0.493	70	1.28	0.8
2	22.26	0.1691	35	2.4	0.53	75	1.2	0.85
3	16.5	0.1964	40	2.14	0.567	80	1.13	0.89
4	13.31	0.2188	45	1.93	0.604	85	1.06	0.94
6	9.79	0.2552	50	1.75	0.641	90	1	1
8	7.86	0.285	55	1.61	0.678			

From the table, it is possible to determine m and n:

m=1.13

n=0.89

These values are changed with change of wheel radiuses. Effects of variations of wheel radiuses are presented in table 4.1, 4.2 and 4.3.

Then, the elliptical contact patch parameter a and b are calculated to determine the maximum pressure in the contact area. The value of the two elliptical contact parameters are differ due to different applied loads and at the same time the maximum contact pressure also changed. To find a and b it is must to know the applied load in individual wheel.

So, depending on the working condition of the train, we can determine the applied load as follows referring the above table which is passenger capacity table from AALRT loading conditions.

3.7.1. Calculation of Maximum Pressure for Passenger Wheel CL60 and U74 Rail

- R_{1w} is considered as wheel contact curvature = 1098mm
- R_{2w} is considered as the major rolling radius of the wheel = 330mm
- R_{2r} is considered as rail contact curvature = 300mm
- R_{1r} as the major rolling radius of the rail = ∞

In the case of AW0 Empty Weight (Load = 44,000kg);

To calculate the applied load at each wheel in the train, multiply the vehicles empty weight with earth's gravity and divide it by number of wheels in that the vehicle have (in this case use vehicles empty weight).

$$Fn = \frac{mass * gravity}{no.of\ wheels\ in\ axle} \quad \text{.....3.10}$$

$$Fn = \frac{44{,}000 * 9.81}{12}$$

Fn= 35,970N, applied load in a wheel

The semi-elliptical contact patch parameters can be calculated using the following formals. To use the following formulas the mechanical properties of the wheel and rail which are elastic modules, poisons ratio and the applied load in the wheel are consider. Also, parameters which are wheel radius, wheel contact curvature at the contact point and rail contact curvature at the contact point are considered.

Using Equation (3.5) and Equation (3.6)

$$(\frac{a}{m})^3 = \frac{3\pi Fn(\delta w + \delta r)}{4(A+B)}$$

$$\left(\frac{a}{1.13}\right)^3 = \frac{3\pi * 35970 * (1.38 + 1.38) * 10\text{^} - 6}{4(0.00364)}$$

a= 4.53mm

$$\left(\frac{b}{n}\right)^3 = \frac{3\pi Fn(\delta w + \delta r)}{4(A+B)}$$

$$\left(\frac{b}{0.89}\right)^3 = \frac{3 * \pi * 35{,}970 * (1.38 + 1.38) * 10\text{^} - 6}{4(0.00364)}$$

b= 3.56mm

Now it is possible to calculate maximum contact pressures.

Maximum pressure in the contact area is also achieved by using Equation (3.4). In the railway field, the maximum contact pressure is frequently over 1000 MPa. This value is over the elastic limit of most steels. [15]

Using Equation (3.4):

$$Po = \frac{3F}{2\pi ab}$$

$$Po = \frac{3 * 35{,}970}{2\pi * 0.00453 * 0.00356}$$

Po=1059.63 MPa

In the case of AW3 Maximum Permissible Weight; (load =63,020kg)

To calculate the applied load at each wheel in the train, multiply the vehicles weight and passengers load with earth's gravity and divide it by number of wheels in that the vehicle have (in this case use the maximum permissible weight).

$$\text{Fn} = \frac{mass * gravity}{no.of\ wheels\ in\ axle}$$

$$\text{Fn} = \frac{63{,}020 * 9.81}{12}$$

Fn = 51,518.85 N: Applied load in a wheel

To obtain the semi-axes of the contact ellipse a (forward) and b (lateral); using Equations (3.5) and (3.6).

$$\left(\frac{\text{a}}{\text{m}}\right)^3 = \frac{3\pi Fn(\delta w + \delta r)}{4(A+B)}$$

$$\left(\frac{\text{a}}{1.13}\right)^3 = \frac{3\pi * 51519(1.38 + 1.38) * 10\text{^} - 6}{4(0.00364)}$$

a= 5.1 mm

$$\left(\frac{\text{b}}{\text{n}}\right)^3 = \frac{3\pi Fn(\delta w + \delta r)}{4(A+B)}$$

$$\left(\frac{\text{b}}{0.89}\right)^3 = \frac{3\pi * 51519(1.38 + 1.38) * 10\text{^} - 6}{4(0.00364)}$$

b= 4.02 mm

Using Equation (3.4) it is possible to calculate the maximum pressure in the contact area.

$$Po = \frac{3F}{2\pi ab}$$

$$Po = \frac{3 * 51{,}518.85}{2\pi * 0.0051 * 0.00402}$$

Po= 1199.8 MPa

In the case of Overloading; (maximum load =66,800kg)

To determine the applied overload on the train it is better to use other transport sectors data because of the lack of recorded data. For this Anbessa city bus's data can give more satisfaction than others. According to Solomon Kebebew [19] (Analysis of effect of train overload on disc brake of AALRT); the company gives service to the customers with 10 per/m^2 in overloading condition. Therefore:

$$\text{Fn} = \frac{mass * gravity}{no.of\ wheels\ in\ axle}$$

$$\text{Fn} = \frac{66{,}800 * 9.81}{12}$$

Fn = 54,609 N : Applied load in a wheel

To obtain the semi-axes of the contact ellipse a (forward) and b (lateral); using Equations (3.5) and (3.6).

$$\left(\frac{\text{a}}{\text{m}}\right)^3 = \frac{3\pi Fn(\delta w + \delta r)}{4(A+B)}$$

$$\left(\frac{\text{a}}{1.13}\right)^3 = \frac{3\pi * 54{,}609(1.38 + 1.38) * 10\text{^} - 6}{4(0.00364)}$$

a= 5.2 mm

$$\left(\frac{\text{b}}{\text{n}}\right)^3 = \frac{3\pi Fn(\delta w + \delta r)}{4(A+B)}$$

$$\left(\frac{\text{b}}{0.89}\right)^3 = \frac{3\pi * 54{,}609(1.38 + 1.38) * 10\text{^} - 6}{4(0.00364)}$$

b= 4.1 mm

Using Equation (3.4) it is possible to calculate the maximum pressure in the contact area.

$$Po = \frac{3F}{2\pi ab}$$

$$Po = \frac{3 * 54{,}609}{2\pi * 0.0052 * 0.0041}$$

Po= 1222.98 MPa

3.7.2. Passenger Wheel ER7 contact with the same Rail (U74)

Major rolling radius of the wheel = 330mm

Thus, pressure at the contact area will be calculated as the following:

In the case of AW0 Empty Weight (Load = 44,000kg);

a= 4.6 mm

b= 3.59 mm

$$Po = \frac{3F}{2\pi ab}$$

$$Po = \frac{3 * 35{,}970}{2\pi * 0.0046 * 0.00359}$$

Po=1039.99 MPa

In the case of AW3 Maximum Permissible Weight; (load =63,020kg)

a= 5.13 mm

b= 4.1 mm

$$Po = \frac{3F}{2\pi ab}$$

$$Po = \frac{3 * 51{,}518.85}{2\pi * 0.00513 * 0.0041}$$

Po= 1169.52 MPa

In the case of Overloading; (maximum load =66,800kg)

a= 5.3 mm

b= 4.13 mm

$$Po = \frac{3F}{2\pi ab}$$

$$Po = \frac{3 * 54{,}609}{2\pi * 0.0053 * 0.00413}$$

Po= 1191.2 MPa

3.7.3. Passenger Wheel R8T contact with the same Rail (U74)

Major rolling radius of the wheel = 330mm

Contact patches and pressure at the contact area will be calculated as the following:

In the case of AW0 Empty Weight (Load = 44,000kg);

a= 4.55 mm

b= 3.58 mm

$$Po = \frac{3F}{2\pi ab}$$

$$Po = \frac{3 * 35{,}970}{2\pi * 0.00455 * 0.00358}$$

Po=1054.35 MPa

In the case of AW3 Maximum Permissible Weight; (load =63,020kg)

a= 5.126 mm

b= 4.04 mm

$$Po = \frac{3F}{2\pi ab}$$

$$Po = \frac{3 * 51{,}518.85}{2\pi * 0.005126 * 0.00404}$$

Po= 1187.8 MPa

In the case of Overloading; (maximum load =66,800kg)

a= 5.23 mm

b= 4.12 mm

$$Po = \frac{3F}{2\pi ab}$$

$$Po = \frac{3 * 54{,}609}{2\pi * 0.00523 * 0.00412}$$

Po= 1210.06 MPa

The principal stresses at the Centre of the surface of contact are calculated as [18]:

$$\sigma_1 = -2\vartheta p_o - (1 - 2\vartheta) + p_o \frac{b}{a+b} \quad \text{.....3.11}$$

$$\sigma_2 = -2\vartheta p_o - (1 - 2\vartheta) + p_o \frac{a}{a+b} \quad \text{.....3.12}$$

$$\sigma_2 = -p_o \quad \text{.....3.13}$$

The angular velocity of the wheel with maximum operating speed of the vehicle is given as:

$$\omega = \frac{\mathcal{V}}{R1w} \quad \text{.....3.14}$$

The maximum designed operating speed of the vehicle was 70 km/hr., but now a day the AALRT operates on a maximum speed of 60 km/hr.

$$\omega = \frac{16.67\text{m/s}}{0.33m}$$

ω= 50.51 rad/s

Where: - $\mathcal{V}$ is the maximum operation speed of the vehicle, 60 km/hr. = 16.67 m/s and $R1w$ is the principal rolling radius of the wheel, 330mm = 0.33m.

3.8. Wheel/Rail Modeling and Analysis

In order to build a realistic model of wheel/rail contact problem a 3D wheel and rail model is needed. This model should be able to accurately calculate the stress response in the contact region. The model is constructed by CATIA V5R19 software and imported to ANSYS 14.5 workbenches.

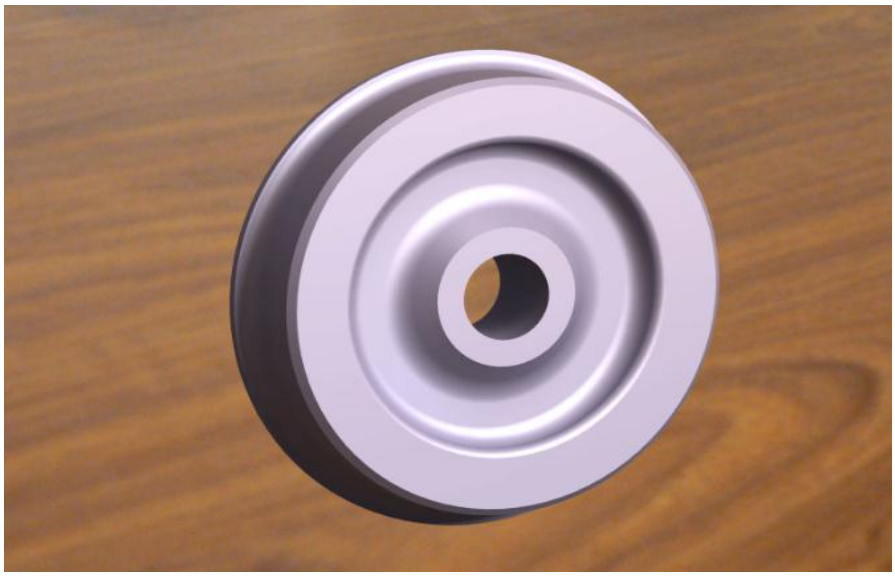

Figure 3. 12 Model of the wheel

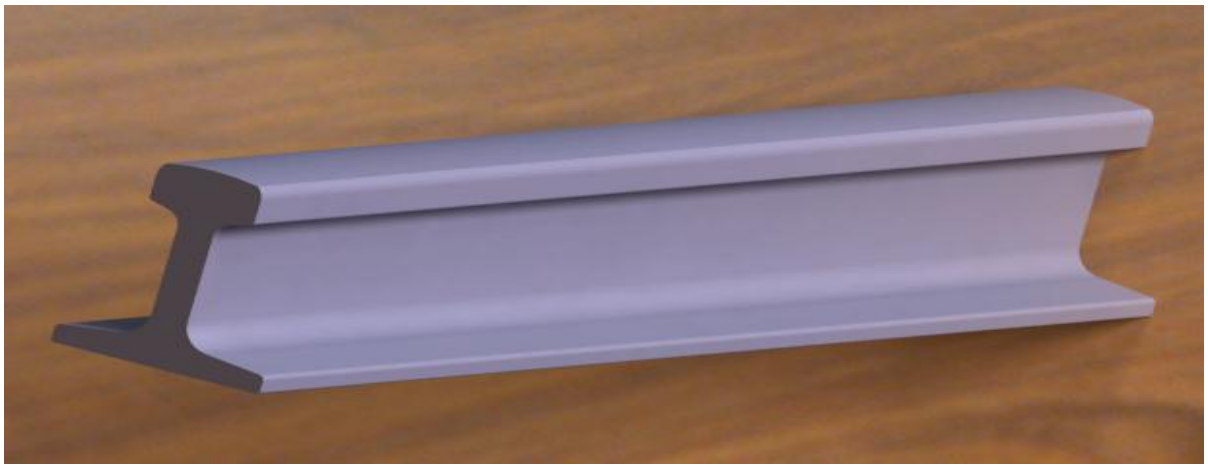

Figure 3. 13 Model of the rail.

3.8.1. ANSYS Procedure for Contact Analysis

According to Gaurav Saini, Dr. Tilak Raj and Arnav Sharma [20] the ANSYS Procedure for Contact Analysis are as follows.

- File of the wheel and track is saved in IGS format.
- 3D model of wheel and track assembly is inserted in ANSYS.
- Then simulation option is selected for analysis of wheel and track.
- Connection is made between wheel and rail by connections in project tree.
- Rough Contact between wheel and rail is selected by contact option.
- Tetrahedral element is selected in Meshing method under mesh and mesh is generated.
- Track is fixed in all 3 DOF by fixture option.
- Load is applied on wheel. Stress result is obtained by showing the final result option.

3.8.1.1. Static Structural Analysis of Wheels

The 3D model of the railway wheel and rail are created using CATIA V5R19 software package. The modeled wheel used in the analysis is the same for different case. But the wheels are different in material chemical composition and mechanical properties, and not in structural dimensions.

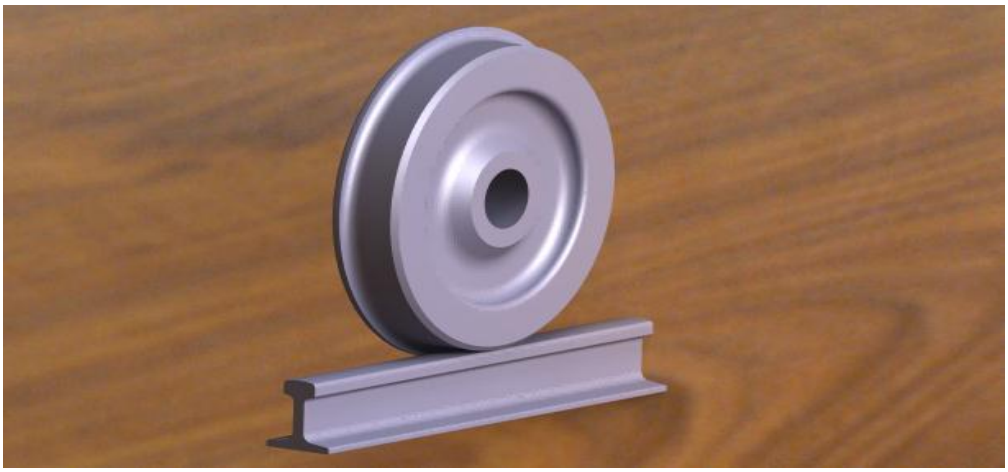

Figure 3. 14 Wheel/rail modeling using CATIA V5R19 software

3.8.1.2. Meshing

In the finite element analysis the basic concept is to analyze the structure, which is an assemblage of discrete pieces called elements, which are connected together at a finite number of points called nodes. A network of these elements is called as a mesh. For this analysis, automatic mesh generating are used in ANSYS rather than defining the nodes individually, after importing the wheel/rail model to ANSYS workbench.

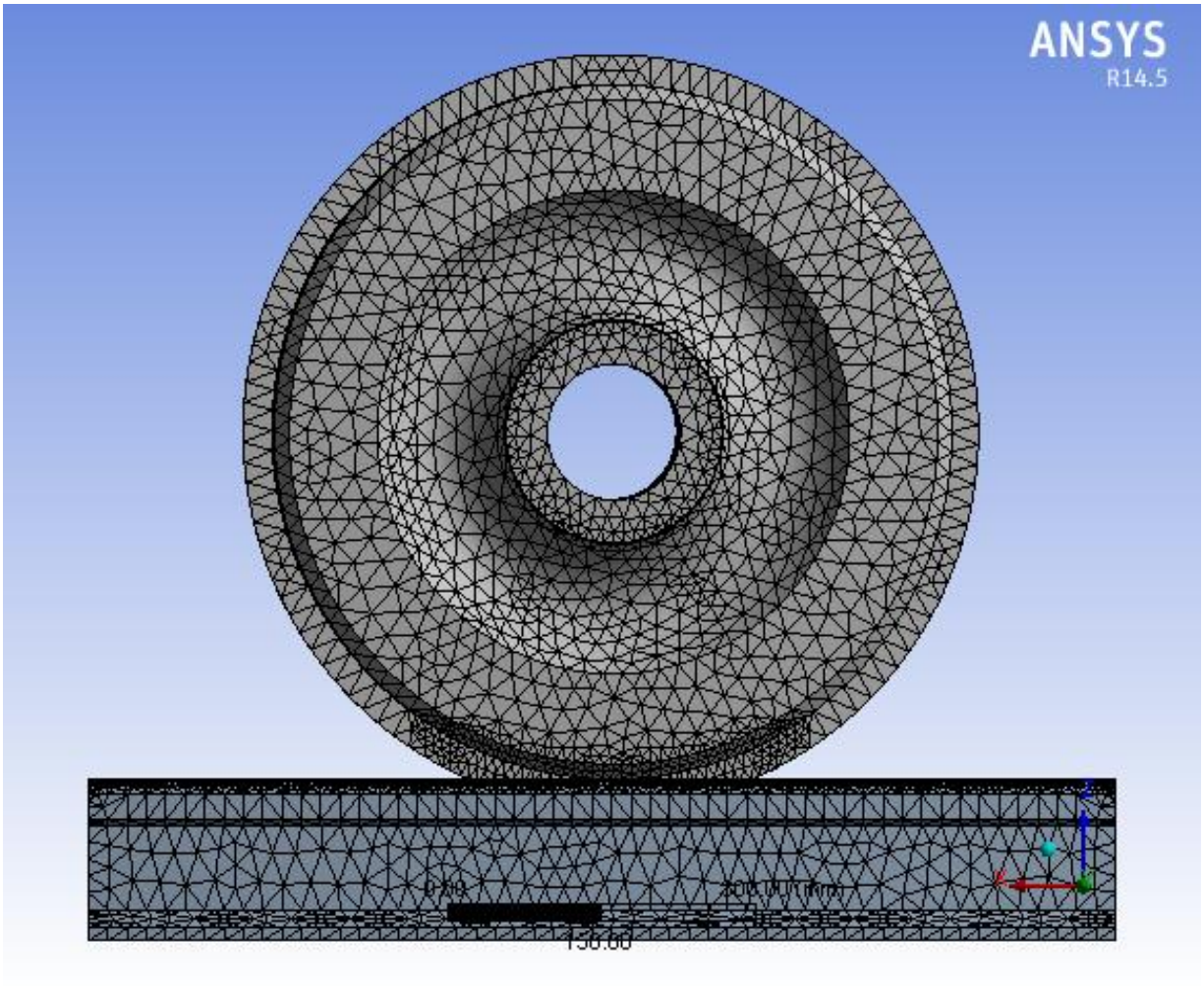

Figure 3. 15 Wheel/rail meshing in ANSYS workbench

3.8.1.3. Definition of the Applied Load and Fixed Support

After completion of the finite element model and mesh, it is necessary to apply constraints and loads to the model. The analyzed railway wheel with rail was subjected applied load on the wheel center. The analysis is going to be done for different loads with different wheel material. The applied load is the same for the first wheel (CL60), second wheel (ER7) and third wheel (R8T), since the wheels are going to be analyzed with the same applied overload. And track is fixed in all 3 DOF.

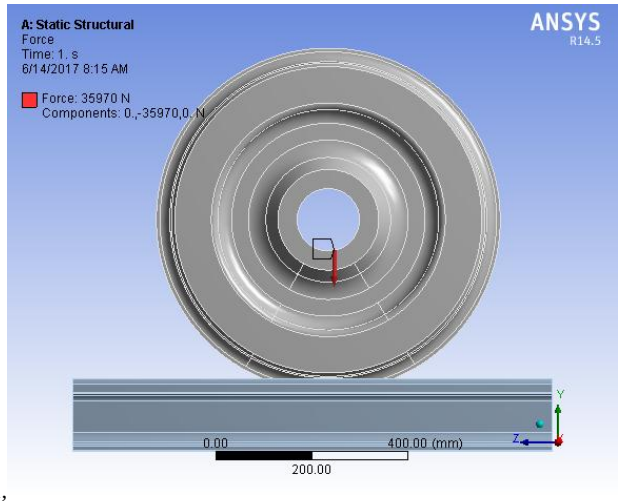

a_1,

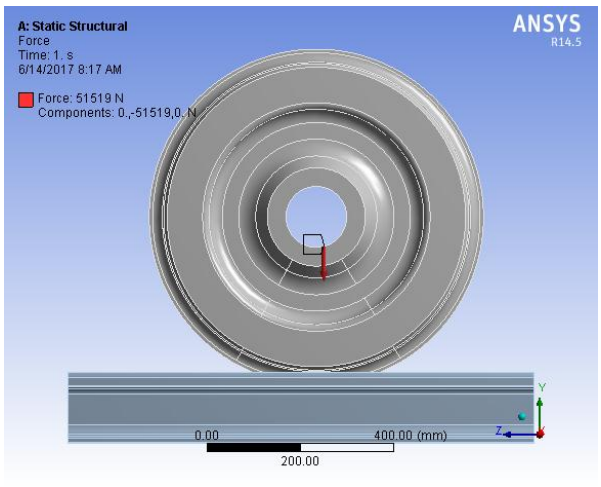

a_2,

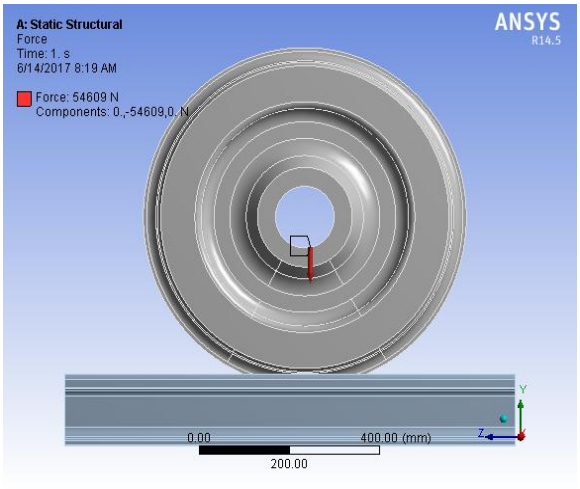

a_3,

(a_1): applied load in the case of AW0 Empty Weight; (a_2): applied load in the case of AW3 maximum permissible Weight; (a_3): applied load in the case of overloading

(b)

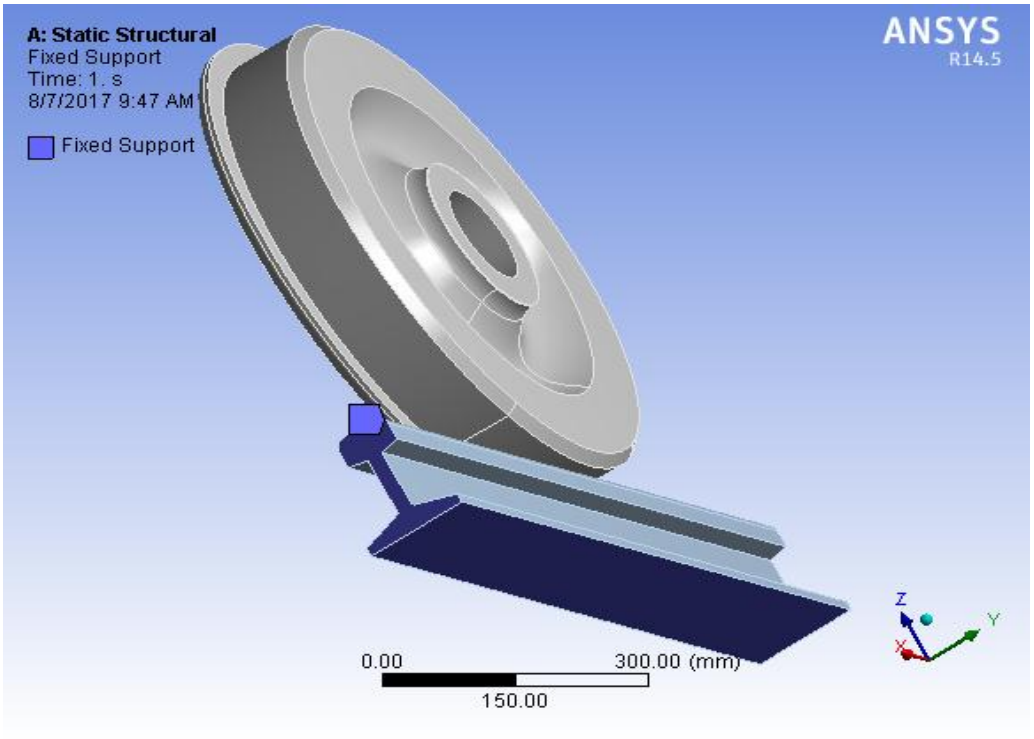

(c)

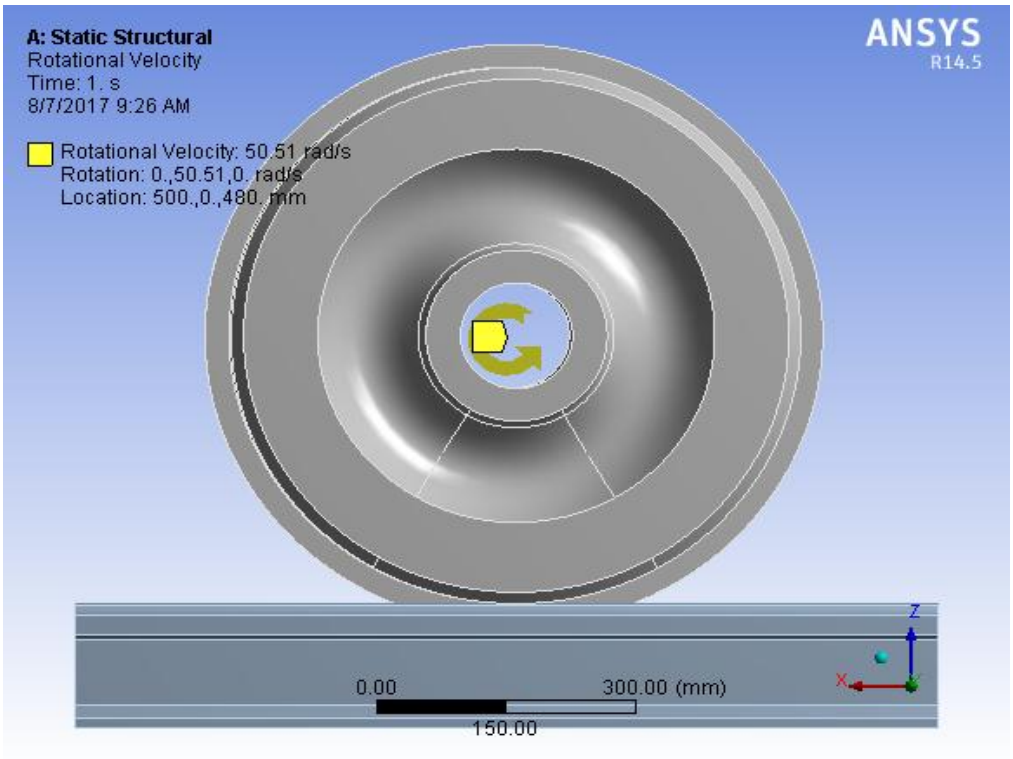

Figure 3. 16 (a) Load applied on wheel center and (b) fixed the track (c) rotational velocity

CHAPTER FOUR

RESULTS AND DISCUSSIONS

The focus of this paper is on the Analysis of the Influences of Train Overloading on Wheel Surface Damage in AALRT and selecting a better wheel material which can resist the current AALRT loading conditions. The contact stresses between wheel and rail can be estimated with the ANSYS analysis; also deformation, fatigue life and fatigue damage of the materials are analyzed. Three different materials of wheels are considered. The wheels are differing in material (mechanical properties and chemical compositions) but have the same profile and size.

Wheels are subjected high stress, strain and deformation in contact with rails. The occurrence of high stress on the wheel is one of the reasons of failures. Wheel surface damage of the part has negative impact on vehicle performances.

The above Equations (3.1 to 3.14) are used to calculate the contact dimension (patch), contact pressure and stress between wheel-rail contact pair with varying applied load. The wheel – rail structures and profiles used in the present study is as per ERC Railway standards.

The variations of applied loads are considered from empty load to overloading conditions. The wheel-rail model is linear-elastic. The contact loads are taken as 35970N to 54609N. Material data Ewheel=210 GPa, Erail=210 GPa, $\boldsymbol{\nu}$wheel & $\boldsymbol{\nu}$rail=0.3 for AALRT, Ewheel=206 GPa, Erail=210 GPa, $\boldsymbol{\nu}$wheel =0.27 & $\boldsymbol{\nu}$rail=0.3 for ER7 and Ewheel=206 GPa, Erail=210 GPa, $\boldsymbol{\nu}$wheel =0.285 & $\boldsymbol{\nu}$rail=0.3 for R8T. Also the different contact parameters, R_{1w}=1098 mm, R_{2w}=330, R_{1r}=∞, R_{2r}=300 mm are used.

The effects of wheel radius are present on table 4.1 to 4.3 and the ANSYS results are present on appendix part.

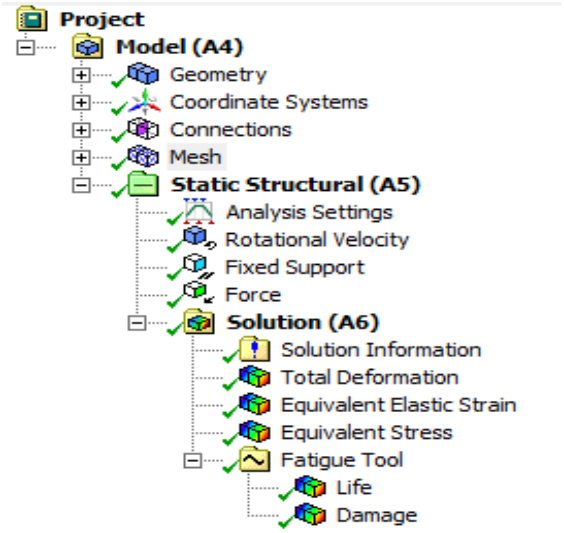

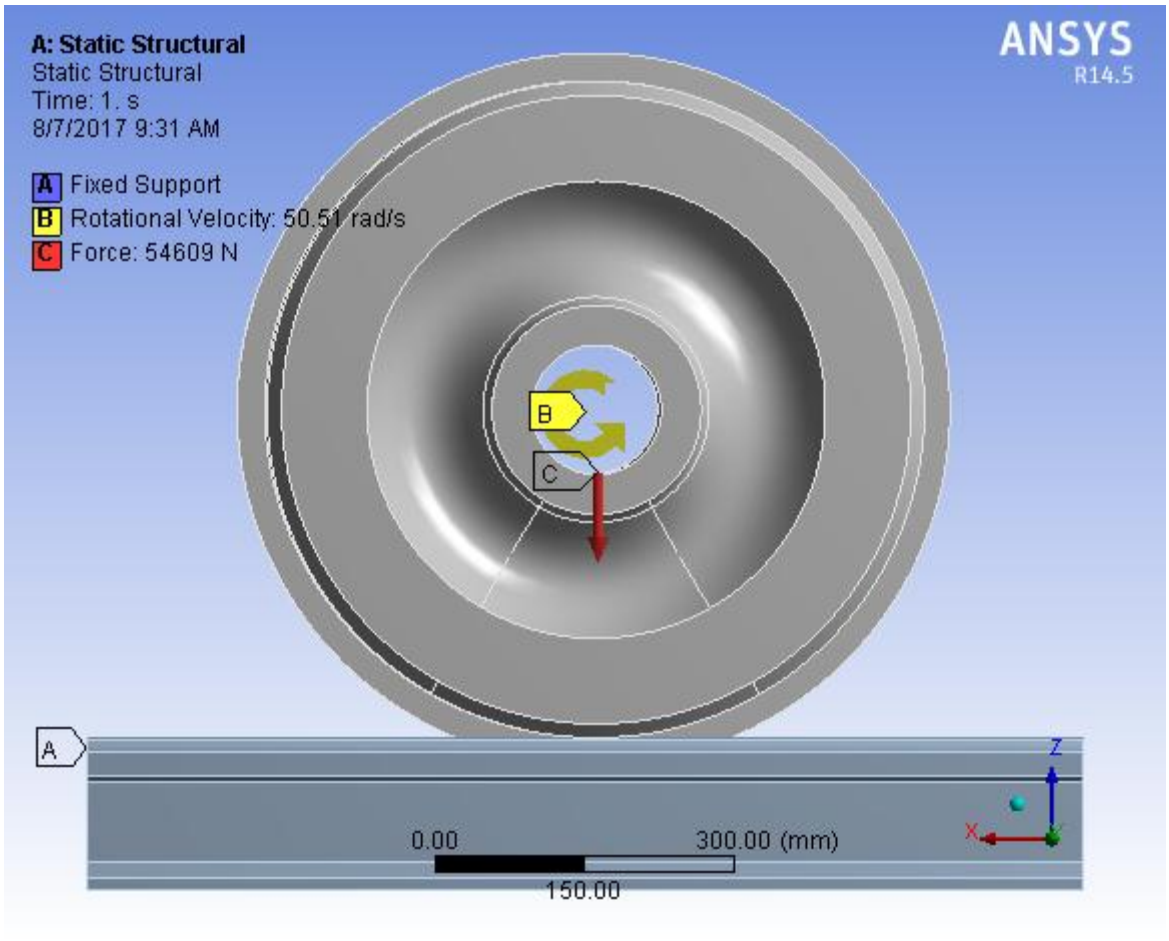

Figure 4. 1 Static structural

4.1. Effect of change of wheel radius on contact pressure and stress

The effects of variations of wheel radius are shown on table (4.1, 4.2 & 4.3). Due to the decrement of wheel radiuses the contact patch lateral axis is decreased and the longitudinal axis increases. But in general case the size of the contact area decreases when the wheel radius decreases. As shown in table below the contact pressure and stress increases when the wheel radius decreases with applying the same load. This shows that the occurrence of high pressure and stress on the contact area also depends on the wheel radius and it increases the possibility of wheel wear.

Table 4. 1 Effect of variations of wheel radius in CL60

Wheel radius (mm)	Applied load (N)	Contact patch (mm)		Hertz coefficients		Pressure (MPa)	σ_1 (MPa)	σ_2 (MPa)	σ_3 (MPa)
		a	b	m	n				
330	54609	5.2	4.1	1.13	0.89	1222.98	949.5	1007.3	1222.9
320	54609	5.1	4.142	1.112	0.903	1234.3	961.9	1013.03	1234.3
310	54609	5.015	4.161	1.0992	0.912	1249.5	976.3	1022.9	1249.5
300	54609	4.933	4.2	1.086	0.9214	1258.48	986.6	1026.9	1258.5
290	54609	4.8	4.25	1.06	0.94	1278.13	1006.9	1038.04	1278.1

Table 4. 2 Effect of variations of wheel radius in ER7

Wheel radius (mm)	Applied load (N)	Contact patch (mm)		Hertz coefficients		Pressure (MPa)	σ_1 (MPa)	σ_2 (MPa)	σ_3 (MPa)
		a	b	m	n				
330	54609	5.3	4.13	1.13	0.89	1191.2	883.23	951.22	1191.2
320	54609	5.133	4.2	1.112	0.903	1209.4	903.43	993.03	1209.4
310	54609	5.05	4.21	1.0992	0.912	1229.32	920.6	972.56	1229.32
300	54609	5.0	4.212	1.086	0.9214	1238.1	928.98	977.7	1238.1
290	54609	4.82	4.3	1.06	0.94	1258.03	952.2	985.2	1258.03

Table 4. 3 Effect of variations of wheel radius in R8T

Wheel radius (mm)	Applied load (N)	Contact patch (mm)		Hertz coefficients		Pressure (MPa)	σ_1 (MPa)	σ_2 (MPa)	σ_3 (MPa)
		a	b	m	n				
330	54609	5.23	4.12	1.13	0.89	1210.06	919.01	980.78	1210.06
320	54609	5.125	4.16	1.112	0.903	1222.98	932.71	987.37	1222.98
310	54609	5.038	4.18	1.0992	0.912	1238.14	947.16	996.72	1238.14
300	54609	4.96	4.205	1.086	0.9214	1250.14	959.22	1003.5	1250.14
290	54609	4.812	4.27	1.06	0.94	1268.97	979.86	1012.42	1268.97

As presented in tables 4.1 to 4.3 the three materials have different results by resisting the applied loads. As shown in the above tables stress and pressure are high in CL60, R8T and ER7 wheels respectively. That means due to the applied loads high stress on the contact area is occurred in CL60 and low in ER7. Due to this the next discussion parts are mainly focused on CL60 wheel materials and ER7 wheels. But the results of R8T wheels are presented.

Equivalent stress

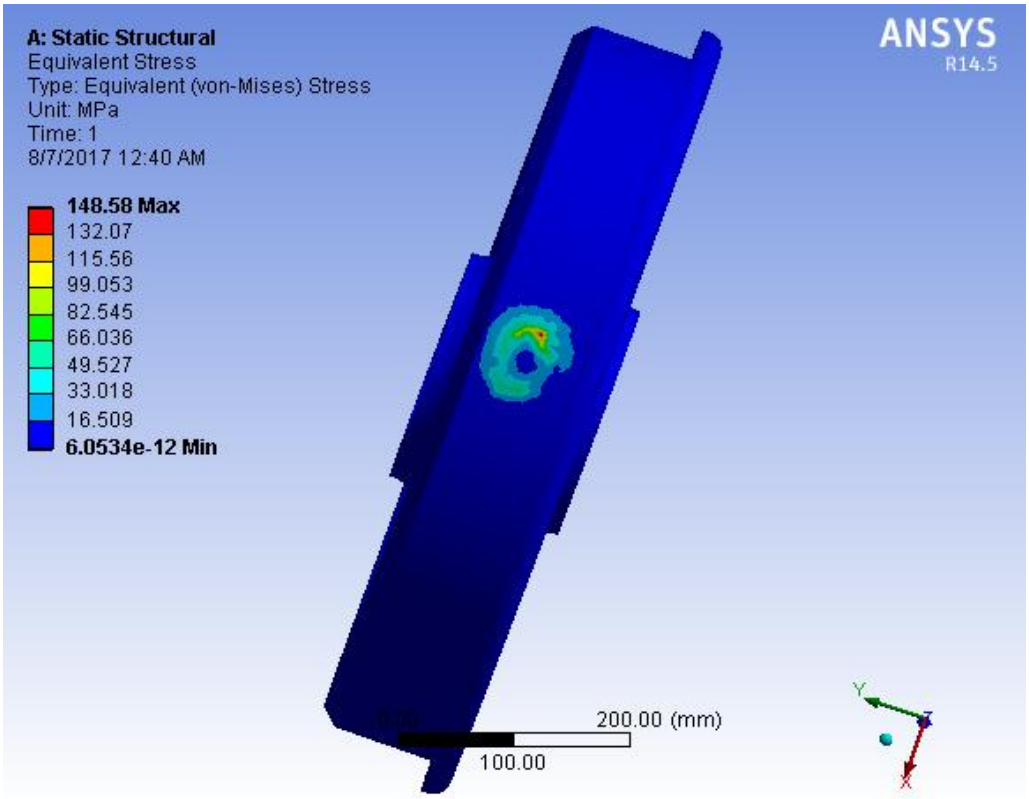

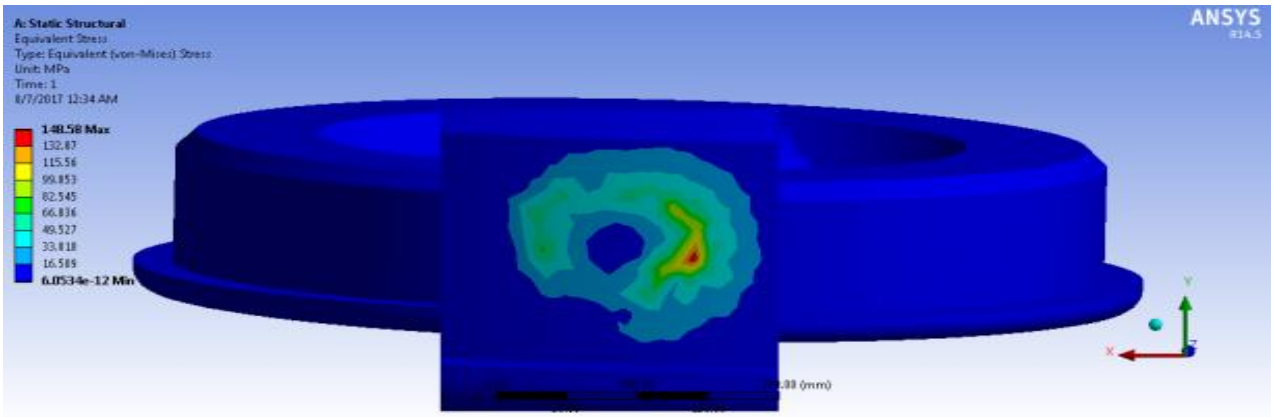

Results	
Minimum	6.0534e-012 MPa
Maximum	148.58 MPa
Minimum Occurs On	Solid

Figure 4. 2 Overloaded Equivalent stress For CL60

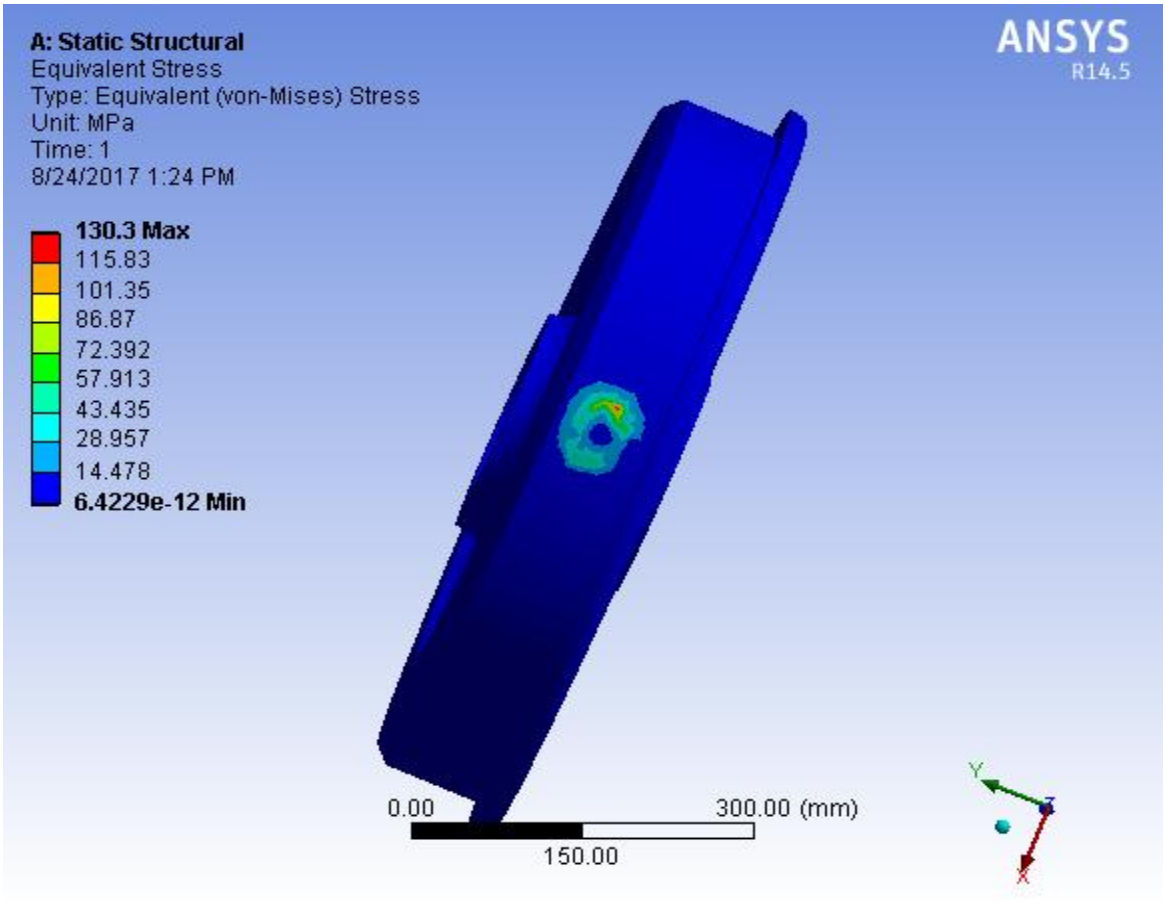

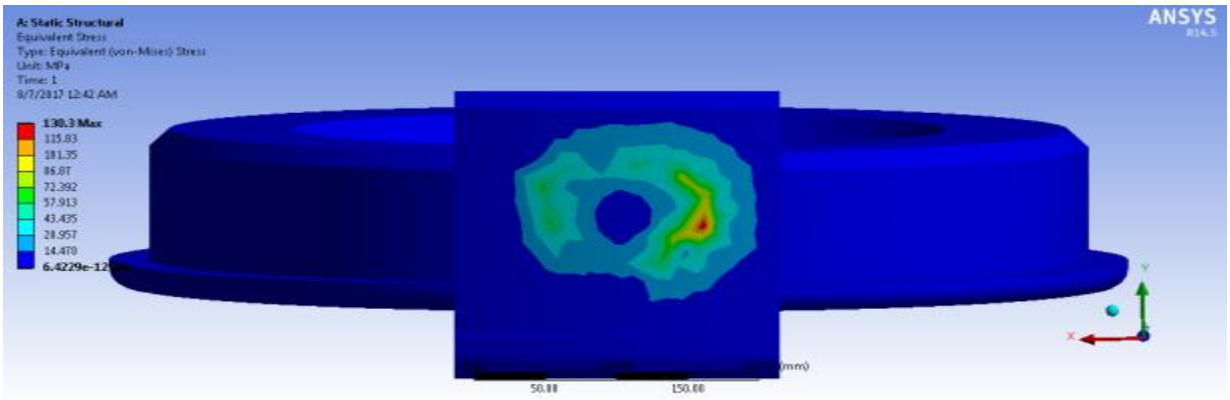

Results	
Minimum	6.4229e-012 MPa
Maximum	130.3 MPa
Minimum Occurs On	Solid

Figure 4. 3 Overloaded Equivalent stress For ER7

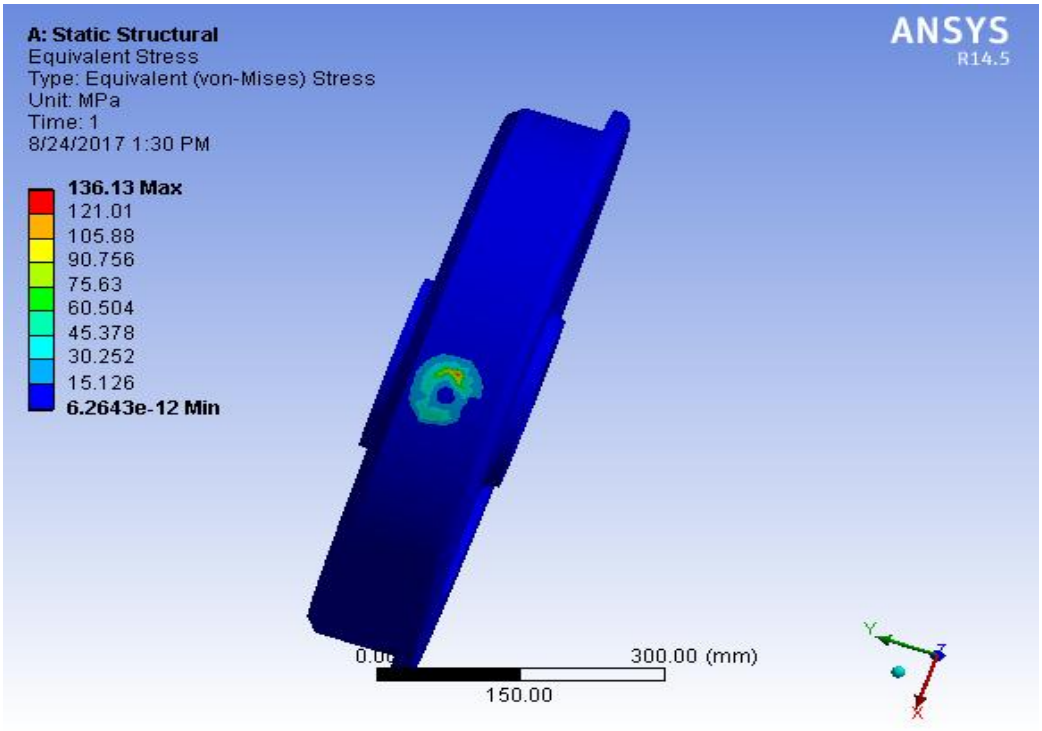

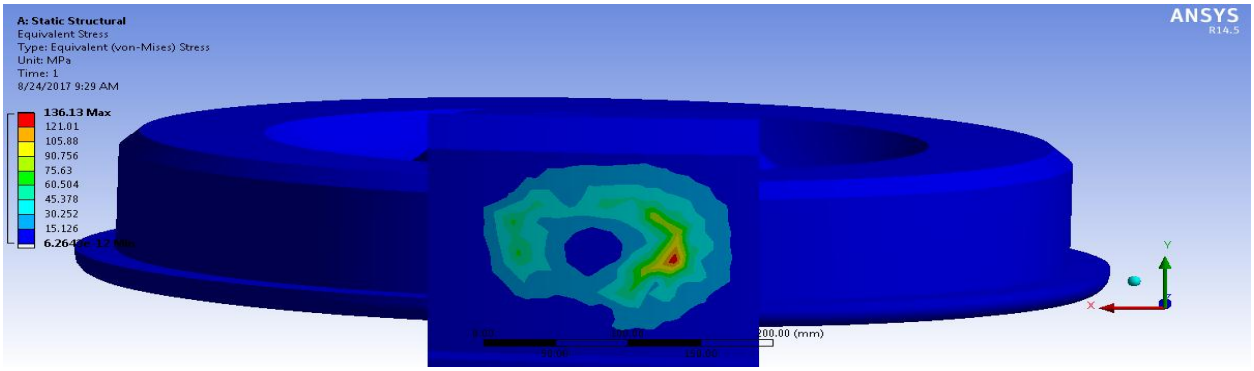

Results	
Minimum	6.2643e-012 MPa
Maximum	136.13 MPa
Minimum Occurs On	Solid

Figure 4. 4 Overloaded Equivalent stress For R8T

The above figures shows that the contact stresses on different three wheel materials (CL60, ER7 and R8T); and high stresses are observed in the current wheel (CL60).

4.2. Effect of applied loads on wheel fatigue life

The load which applies on the wheel increases the contact pressure and stress. When high contact pressure and stress occurs on the contact area between wheel and rail the fatigue life of the materials are decreased. The figures below (4.5, 4.6 and 4.7) shows that the fatigue life of CL60 and ER7 wheels. From the results ER7 wheel has more life than CL60 wheel. This happens because of the materials chemical and mechanical properties.

The increasing of applied load on the wheel contact with rail reduces the fatigue life of the wheel and it generates high friction on the contact area which leads to material wear.

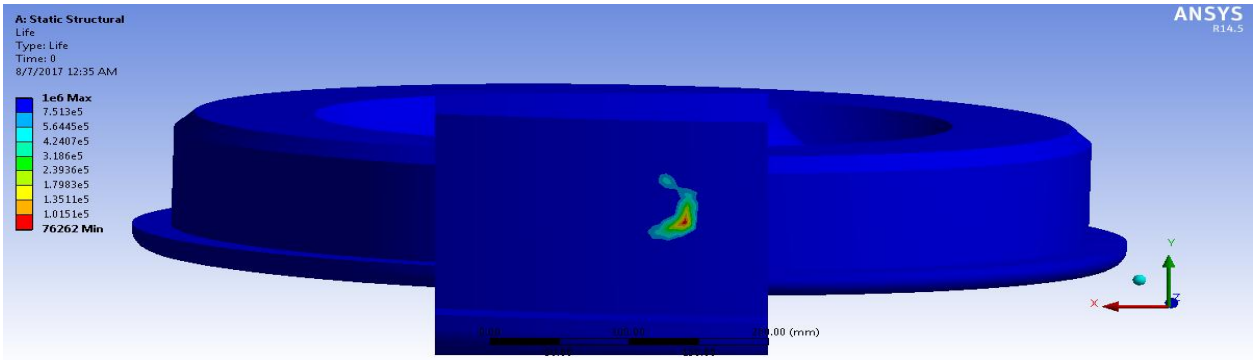

Results	
Minimum	76262 cycles
Minimum Occurs On	Solid

Figure 4. 5 Overloaded fatigue life For CL60

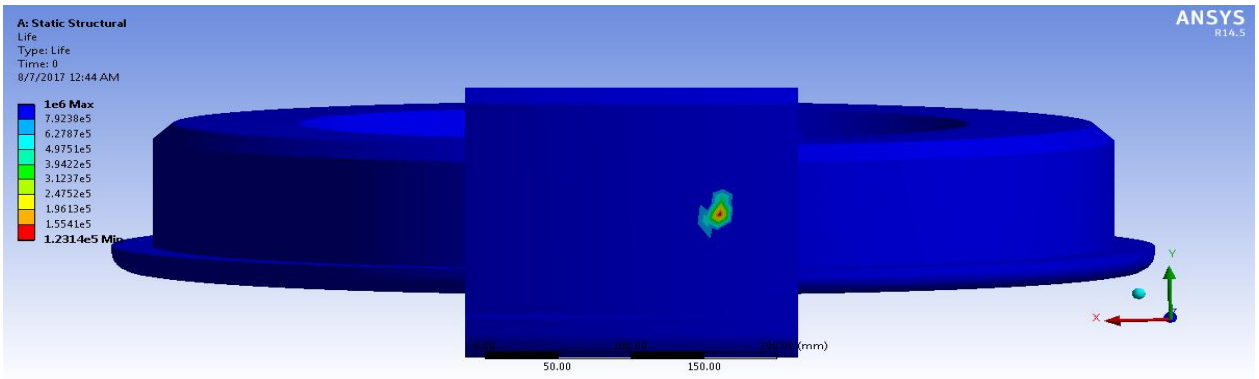

Results	
Minimum	1.2314e+005 cycles
Minimum Occurs On	Solid

Figure 4. 6 Overloaded fatigue life For ER7

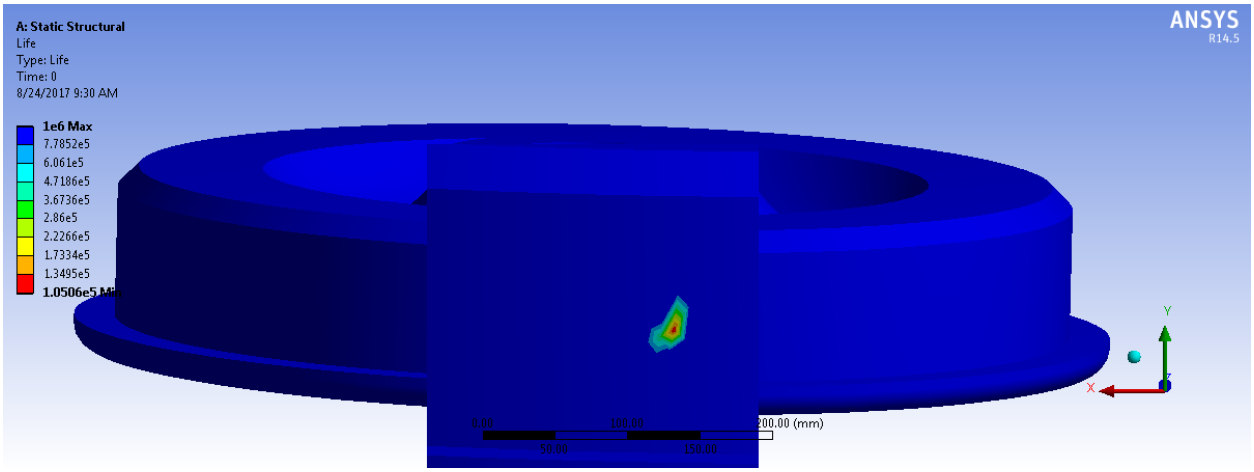

Results	
Minimum	1.0506e+005 cycles
Minimum Occurs On	Solid

Figure 4. 7 Overloaded fatigue life For R8T

As stated before; the fatigue life of wheels is decreased due to the increasing of applied loads. This is shown on the two wheels which apply loads from empty to overloaded conditions. This fatigue life analysis shows that the differences of the two wheel materials by having long life services. Fatigue life methods are aimed to determine the life (number of loading cycles) of an element until failure. [21]

From the results (table 4.4); in the case of AW0 (empty weight) the minimum fatigue life of CL60 wheel is 101,920 cycles which is less than ER7 wheel life by 63,370 cycles (165,290-101,920 = 63,370) This also the same in other cases (maximum permissible load and overloading conditions).

It shows that if the applied load on the wheel becomes high, the life cycle of the wheel is decreased. Specially; on the contact area which has high stress. The decrement of fatigue life with the increasing of contact stress shows that the possibility of failure is becoming high.

Depending on the results it is possible to say that ER7 has more life cycles than CL60 by resisting the applied load. To show this it is better to see the following graphs and relations.

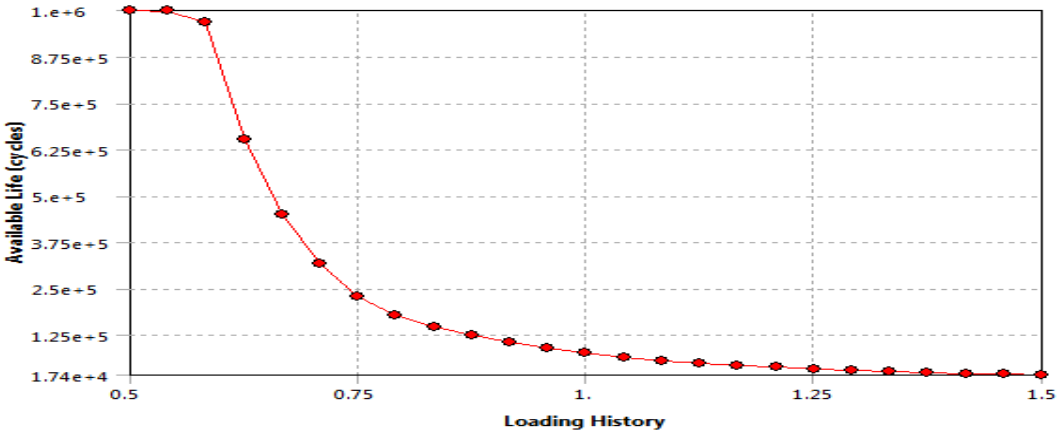

a) CL60 wheels

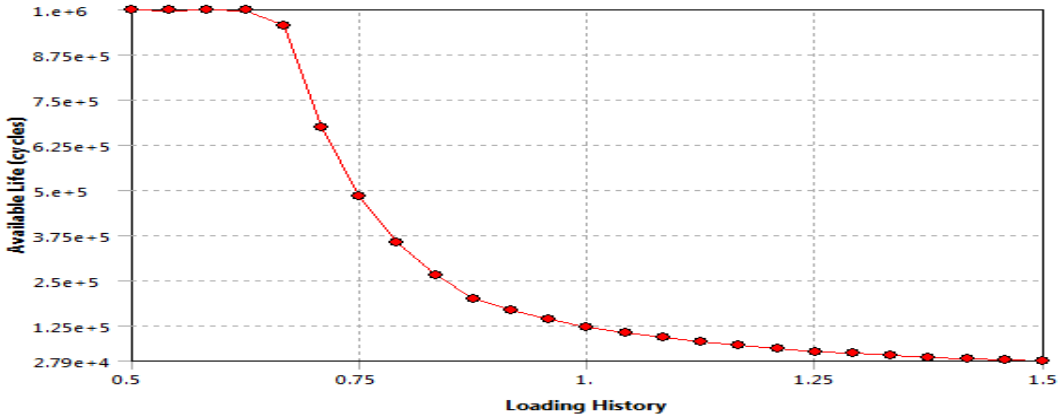

b) ER7 wheels

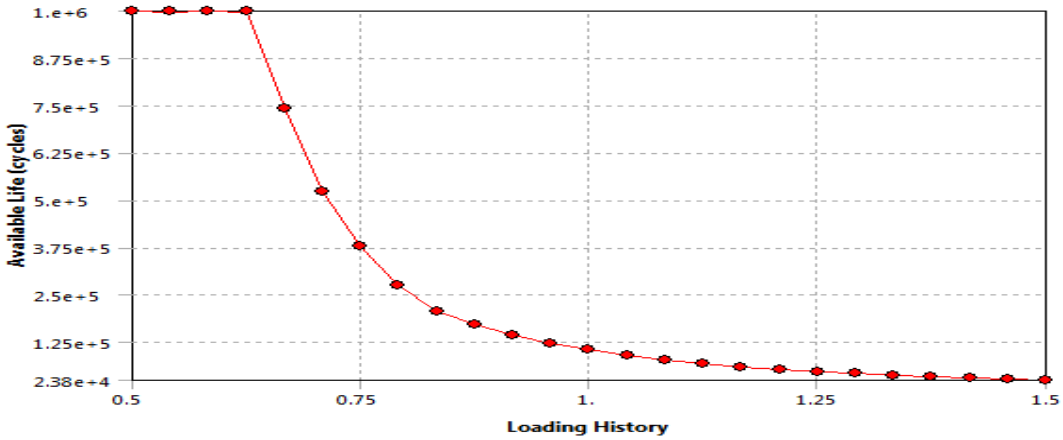

c) R8T wheels

Figure 4. 8 Available Life (cycles) Vs. Load for a) CL60, b) ER7 & c) R8T wheels

Table 4. 4 Fatigue life (cycles)

	Fatigue life (cycles)		
	Load 1 (AW0)	**Load 2 (AW3)**	**Load 3 (overload)**
CL60	101,920	79,906	76,262
ER7	165,290	129,130	123,140
R8T	139,780	110,000	105,060

165,290- 101,920 = 63,370 cycles

CL60=0.6166ER7

129,130- 79,906 = 49,224 cycles

CL60=0.6188ER7

123,140- 76,262= 46,878 cycles

CL60=0.6193ER7

In the above wheel life cycle differences, it is possible to see that the ER7 wheel has more life cycles than others. And it can be approximately relate ER7 with CL60 wheel life cycles as CL60 = 0.618ER7.

4.3. Effect of applied load on wheel deformation

Deformation is the changes in materials dimensions in response to mechanical forces. The increasing of load causes increasing deformation and moves the part closer to failure. As shown in figures (4.8, 4,9 & 4.10) due to the increasing of applied loads on the contact area the deformation of the materials becomes high. This deformation is high in CL60 wheel when it compared with ER7. Deformations have a negative impact on material (wheel) performances.

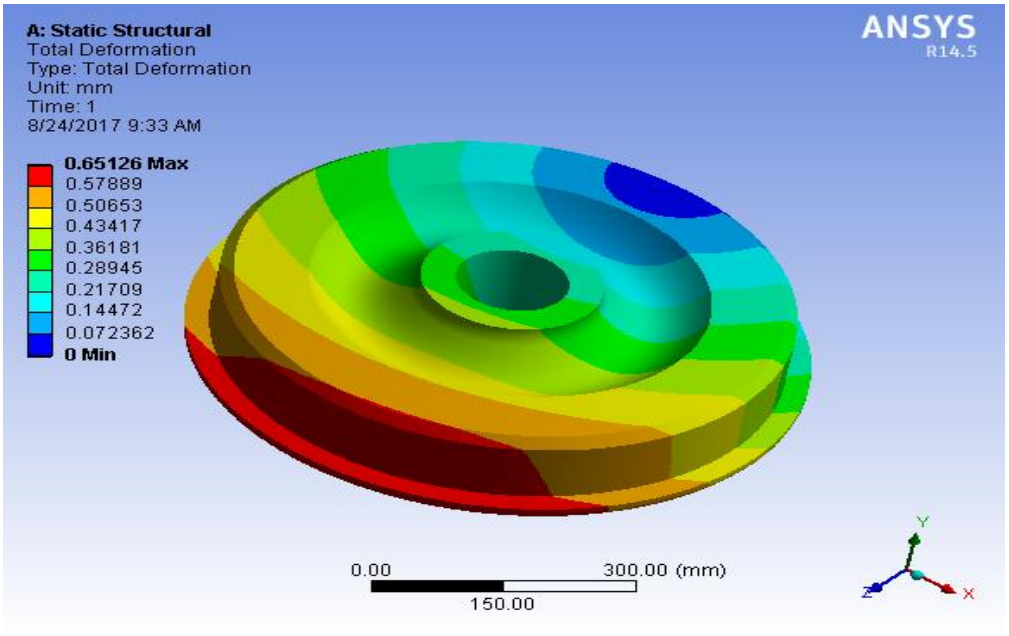

Results	
Minimum	0. mm
Maximum	0.65126 mm
Minimum Occurs On	Solid
Maximum Occurs On	Solid

Figure 4. 9 Overloaded deformation For CL60

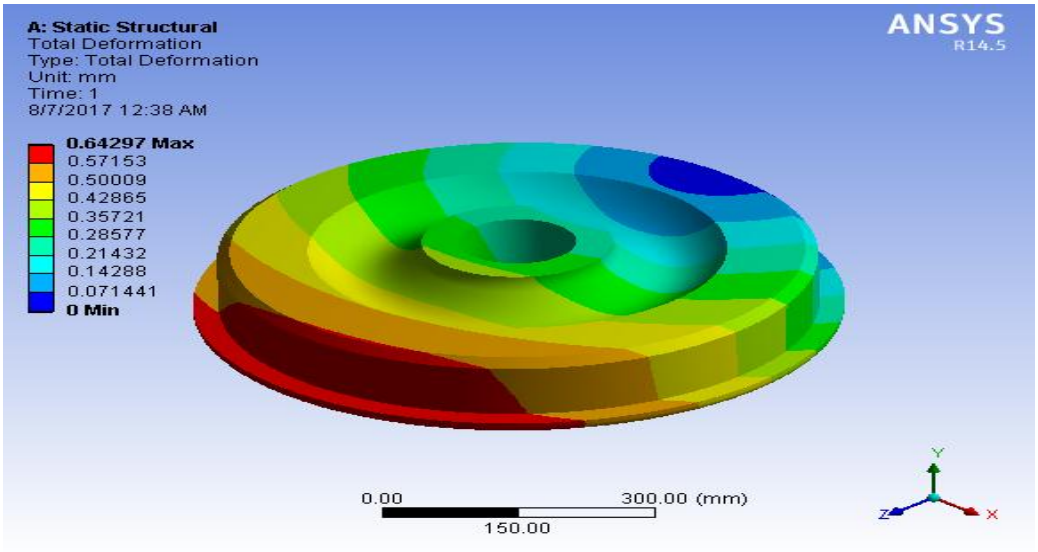

Results	
Minimum	0. mm
Maximum	0.64297 mm
Minimum Occurs On	Solid
Maximum Occurs On	Solid

Figure 4. 10 Overloaded deformation For ER7

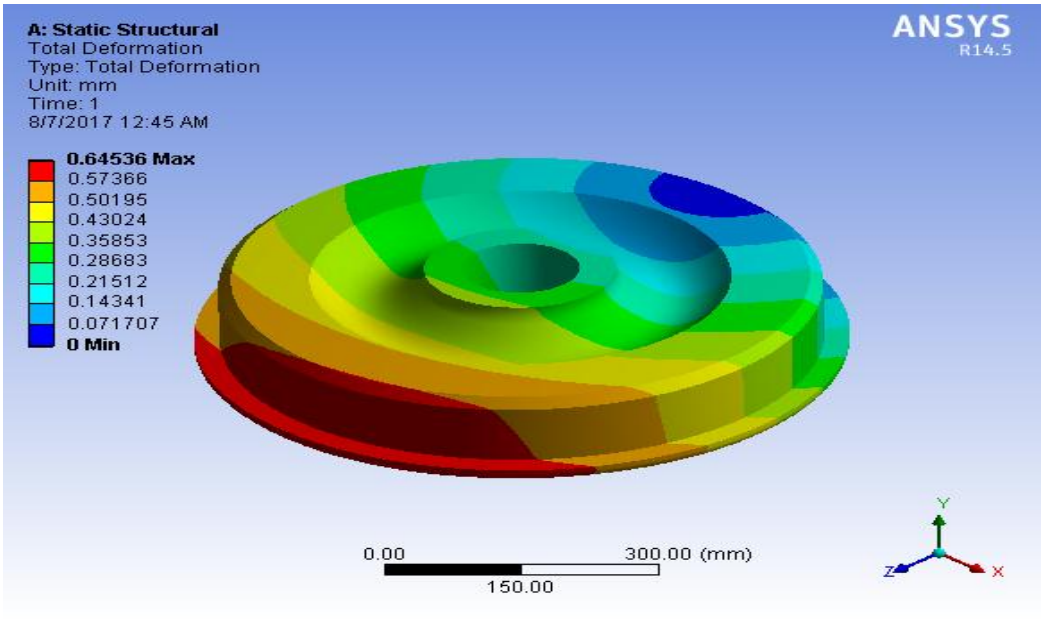

Figure 4. 11 Overloaded deformations For R8T

The stress results show that the current wheel has high stress value than ER7 in the wheel contact with rail. The deformation on the contact area increases with the increasing of applied load on the wheel from empty weight to overloading. This increasing of deformation is greater in wheel CL60 than ER7 wheel.

Table 4. 5 wheels deformation

	Deformation (mm)		
	Load 1 (AW0)	Load 2 (AW3)	Load 3 (overload)
CL60	0.64068	0.64933	0.65126
ER7	0.63322	0.64119	0.64297
R8T	0.63451	0.64339	0.64536

For instance, in the case of overloading the deformation in the current wheel which is CL60 is 0.65126 mm and this deformation is greater than ER7 wheel deformation's by 0.00829 mm (0.65126 - 0.64297 = 0.00829). This shows that ER7 wheel materials have the tendency of resisting the applied load than CL60.

4.4. Fatigue life and deformation

As discussed before the increasing of applied load (high force) increases material deformations and in another hand it decreases the materials fatigue life. The fatigue life of the current wheel CL60 is less than ER7 wheel with the same applied load. This shows that ER7 wheel has the tendency to resist the applied load better than CL60.

Table 4. 6 Fatigue life (cycles) and Deformation

	Fatigue life (cycles) and Deformation (mm)					
	Load 1 (AW0)		**Load 2 (AW3)**		**Load 3 (overload)**	
	Life	Deformation	Life	Deformation	Life	Deformation
CL60	101,920	0.64068	79,906	0.64933	76,262	0.65126
ER7	165,290	0.63322	129,130	0.64119	123,140	0.64297
R8T	139,780	0.63451	110,000	0.64339	105,060	0.64536

From the above table (table 4.6), the life cycles of CL60 in the case of Load 3 is 76,262 cycles, and in this cycle the deformation becomes 0.65126 mm. But in the case of ER7 with the same loading condition the life cycle is 123,140 cycles and the deformation is 0.64297 mm. This shows that the life cycles of ER7 is greater than CL60, however the deformation is less than CL60. And this is also true in other loading conditions. In general, ER7 has more life cycles with less deformation than CL60.

4.5. Equivalent stress and damage

Equivalent stress shows reduction with an increasing of wheel radius (table 4.1, 4.2 and 4.3) and it increases when wheel radiuses are decreased. This increasing of stress decreases the wheel life.

As shown in the figure the wheel fatigue damage increases with the decreasing of wheel fatigue life.

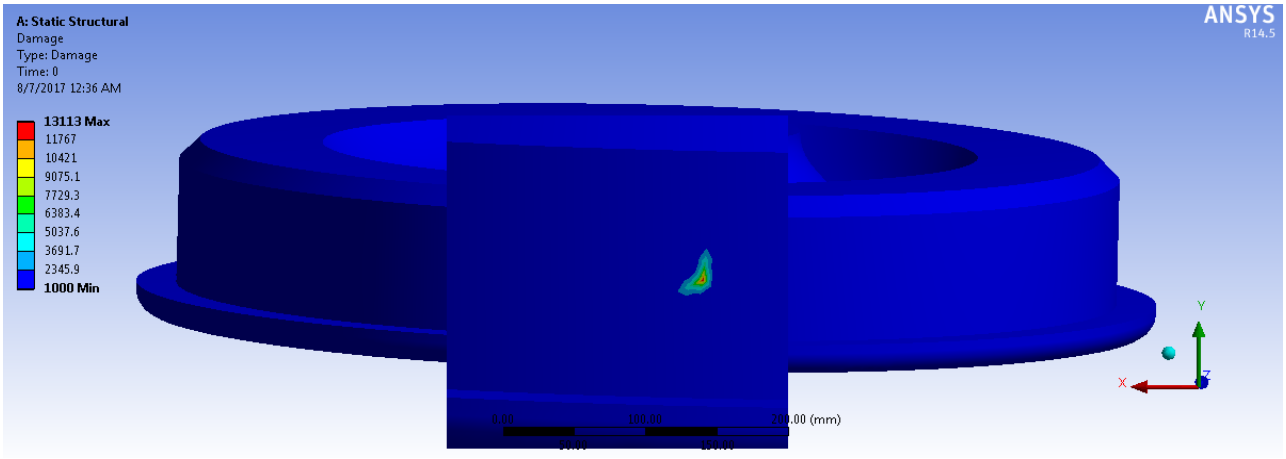

Results	
Maximum	13113
Maximum Occurs On	Solid

Figure 4. 12 CL60 wheel damage

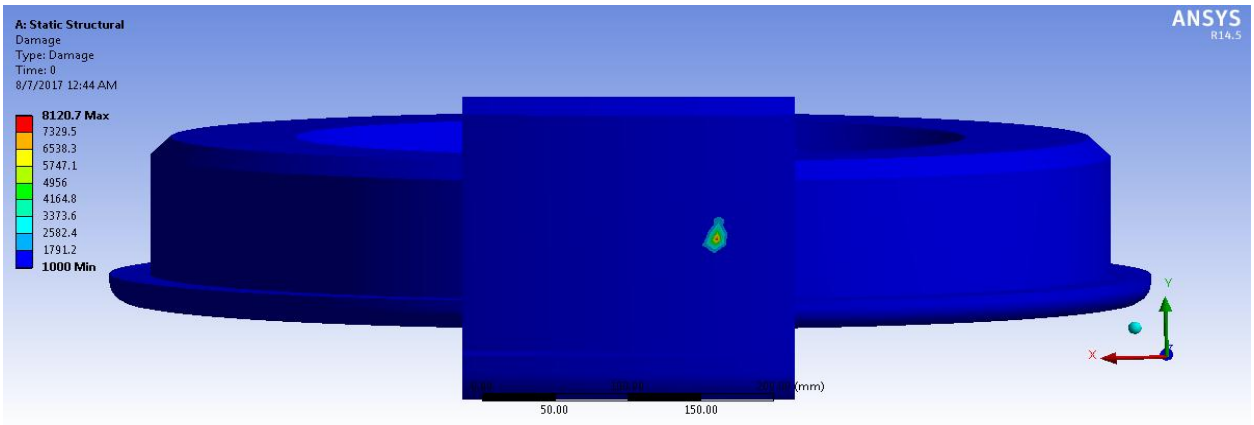

Results	
Maximum	8120.7
Maximum Occurs On	Solid

Figure 4. 13 ER7 wheel damage

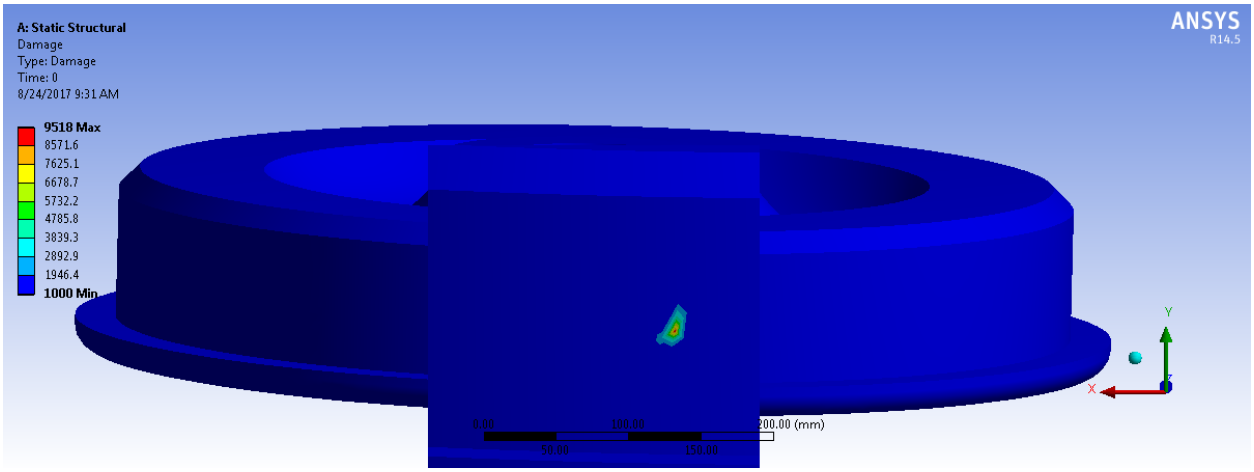

Results	
Maximum	9518.
Maximum Occurs On	Solid

Figure 4. 14 R8T wheel damage

From the above figures (4.11 to 4.13), the fatigue damage in the current wheel CL60 is 13,113 and in ER7 wheel material the fatigue damage is 8,120.7. The differences are around 4992.3 between CL60 and ER7 wheel materials. This shows that the possibility of wheel damage is high in CL60 wheel.

Table 4. 7 Result summary

	Applied load	Contact patch (mm)		Strain (mm/mm) *10^{-3}	Deformation (mm)	Pressure (MPa)	Stress (MPa)	Fatigue life (cycles)	Fatigue Damage
		a	b						
CL60	Empty	4.53	3.56	1.1137	0.64068	1059.63	137.28	101,920	9811.4
	Max. permissible	5.1	4.02	1.1927	0.64933	1199.8	146.7	79,906	12515
	Overloaded	5.2	4.1	1.2084	0.65126	1222.98	148.58	76,262	13113
ER7	Empty	4.6	3.59	1.0068	0.63322	1039.99	120.15	165,290	6050
	Max. permissible	5.13	4.1	1.0778	0.64229	1169.52	128.61	129,130	7744
	Overloaded	5.3	4.13	1.0919	0.64297	1191.2	130.3	123,140	8120.7
R8T	Empty	4.55	3.58	1.0509	0.63451	1054.35	125.83	139,780	7154.2
	Max. permissible	5.126	4.04	1.1251	0.64339	1187.8	134.42	110,000	9090.6
	Overloaded	5.23	4.12	1.1399	0.64536	1210.06	136.13	105,060	9518

CHAPTER FIVE

CONCLUSION AND RECOMMENDATION

5.1. Conclusion

The purpose of this research paper is to analyze the Influences of Train Overloading on Wheel Surface Damage in AALRT. During Train overloading high stress, strain and deformation on the contact point between wheel and rail are occurred. The analysis is done by applying loads on wheels which have the same structural dimension and profile but different mechanical properties.

From the results obtained, high stresses are produced between wheel and rail when the applied loads are increased. The stresses on the contact also increased when the wheel diameters are decreased (table 4.1, 4.2 & 4.3). Because of the occurrence of high stress on the contact area, the fatigue lives of the wheels are decreased but the possibility of deformation and damage on the wheel are increased. These occurrences of deformations and damages are different on the different wheel materials. The fatigue life (76,262) of CL60 wheels are less with high deformation and damage (13,113) compared with ER7 (fatigue life (123,140) and damage (8,120.7)) wheel materials.

ER7 wheel has long life cycles and better resistance of applied loads than that of CL60 wheels. And ER7 wheel may provide improved performances, minimize the sensitivity of overloading and can provide longer life.

5.2. Recommendation

From the analysis and the final conclusion, ER7 wheel material is better than that of CL60 in resisting the applied loads, has less deformation and better fatigue life cycles. So; preferring this wheel has advantages to minimize load sensitivity and providing improved performance. So it is better for Addis Ababa Light Rail Transit (AALRT) to use ER7 wheels.

5.3. Future Works

Under this research paper the effect of overloading on wheel Surface Damage analysis between wheel and rail is done. But in the future the analysis can be performed including the following suggested future works as extensions and elaborations of this research.

- Another additional study by considering different (lateral and longitudinal) forces.
- Analysis considering Environmental effects.
- Investigating the wheel materials chemical compositions and mechanical properties using experimental analysis.
- Study the influence of load by considering track conditions (track gradients, elevations, curves) and so on.
- Investigating other causes (temperature, third particles between wheel and rail/grit) of Surface Damage on the wheel.

REFERENCES

1. Sergey M. Zakharov, Simulation of mutual wheel/rail wears, July 2002.
2. Arthur Anyakwo, Crinela Pislaru, Andrew Ball, A New Method for Modeling and Simulation of the Dynamic Behaviour of the Wheel-rail contact, June 2012.
3. Tanel Telliskivi, Ulf Olofsson, Ulf Sellgren.A tool and a method for FE analysis of Wheel and rail interaction,
4. Ivan Y. Shevtsov, Wheel/Rail Interface Optimization, 2008.
5. C. X. Li, the University of Birmingham, UK
6. Tiberiu axinte, violeta-vali ciucur, Rolling Contact Fatigue. Application in Rail-Wheel Interaction Modeling, Romania,
7. Telliskivi, T. & Olofsson, O. "Contact Mechanics Analysis of Measured Wheel-Rail Profiles Using the Finite Element Method", Proceedings of the Institute of the Mechanical Engineers, Part F: Journal of Rail and Rapid Transit, 2001.
8. Iwnicki, S. "Simulation of Wheel-Rail Contact Forces", Fatigue & Fracture of Engineering Materials and Structures, 2003.
9. Katrin Mädler, Manfred Bannasch Deutsche Bahn AG, "Materials used for Wheels on Rolling Stock", Technical Centre, Brandenburg-Kirchmöser, GERMANY
10. Ulf Olofsson and Roger Lewis, tribology of the wheel rail contact, Taylor and Francis group L.L.C. 2006.
11. Fikru Bekele, the effect of change of wheel-rail contact geometry on contact fatigue stresses, 2014.
12. Ayana Gebremichael, Analysis of Rolling Contact Fatigue Damage and Fatigue Life Comparison of Rail Due to Cyclic Axle Load, 2014.
13. Paul Molyneux-Berry, Claire Davis and Adam Bevan, the Influence of Wheel/Rail Contact Conditions on the Microstructure and Hardness of Railway Wheels, 2014.
14. Roya Sadat Ashofteh, Calculating the Contact Stress Resulting from Lateral Movement of the Wheel on Rail by Applying Hertz Theory, Vol. 6, No. 4 / December 2013.
15. Taylor & Francis Group, LLC Handbook of Railway Vehicle Dynamics**,** 2006

16. S. P. Timoshenko, and J. N. Goodier, Theory of Elasticity, 3rd edition, McGraw-Hill Book Co. Inc., New York, 1970
17. A. Anyakwo, C. Pislaru, A. Ball, A new method for modeling and simulation of the dynamic behaviour of the wheel-rail contact, International Journal of Automation and Computing, 9, 2012.
18. Jay Prakash Srivastava, P.K. Sarkar, Vinayak Ranjan, An Approximate Analysis for Hertzian Elliptical Wheel-Rail Contact Problem, Proceedings of the 1st International and 16th National Conference on Machines and Mechanisms, Dec 18-20 2013
19. Solomon Kebebew, Analysis of Effect of Train Overload on Disc Brake of AALRT, March, 2015.
20. Gaurav Saini, Dr. Tilak Raj, Arnav Sharma, Design and Contact Analysis of Rail Track using Solidworks and Ansys, International Journal of Advanced Technology in Engineering and Science Volume No 03, Special Issue No. 01, April 2015.
21. Dr. Ala Hijazi, Shigley's Mechanical Engineering design, 10th Edition.
22. Oscar arias-cuevas, low adhesion in the wheel-rail contact, Netherlands September 2010.
23. Mingru Zhang and Haicheng Gu, Microstructure and mechanical properties of railway wheels manufactured with low-medium carbon Si-Mn-Mo-V steel, Journal of University of Science and Technology Beijing Volume 15, Number 2, April 2008
24. EN 13262+A1, European standard, Wheelsets and bogies January 2009

APPENDIX

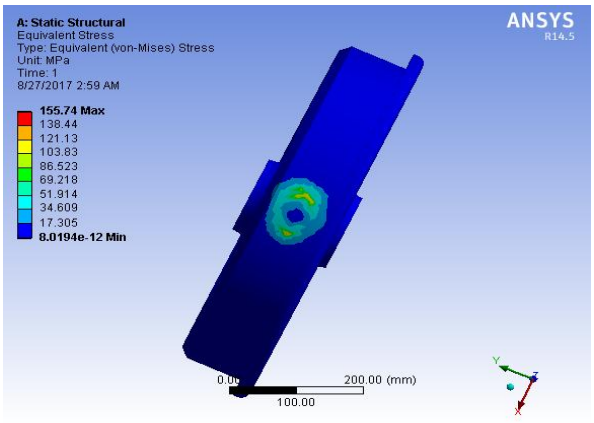

a)

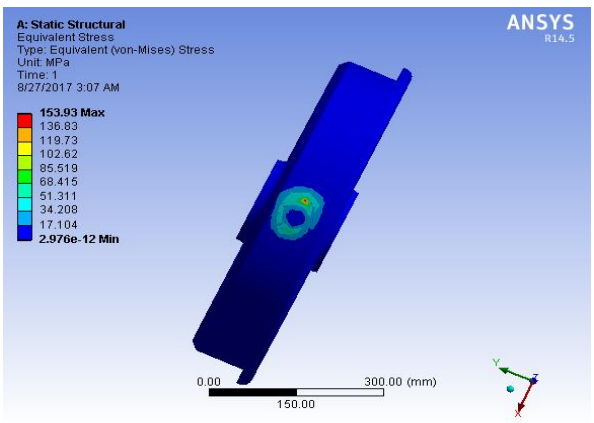

b)

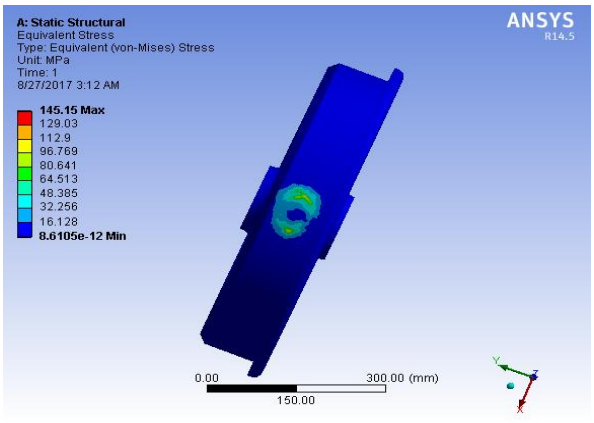

c)

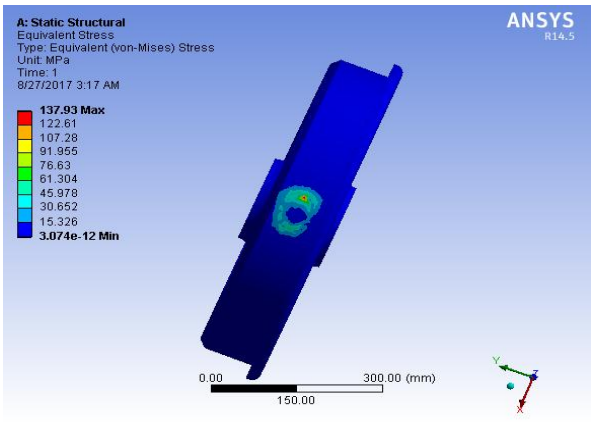

d)

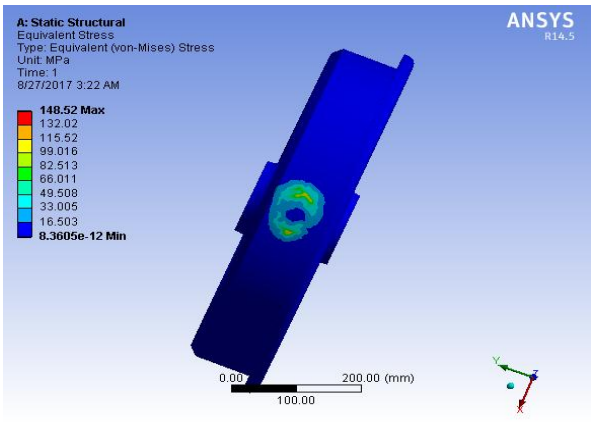

e)

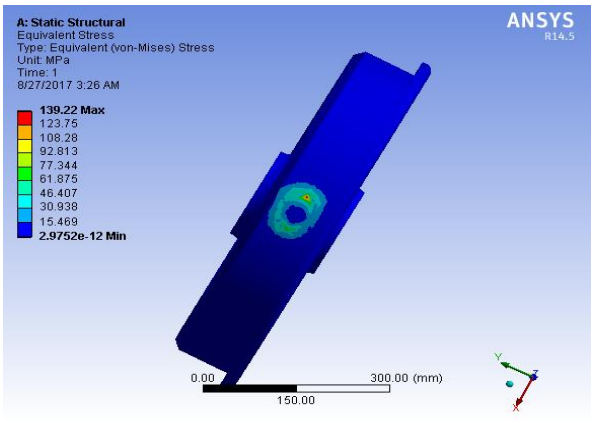

f)

Figure 1: Equ. Stress a,c,e (R_2w 290) & b,d,f (R_2w 310) for CL60,ER7 & R8T wheels respect.

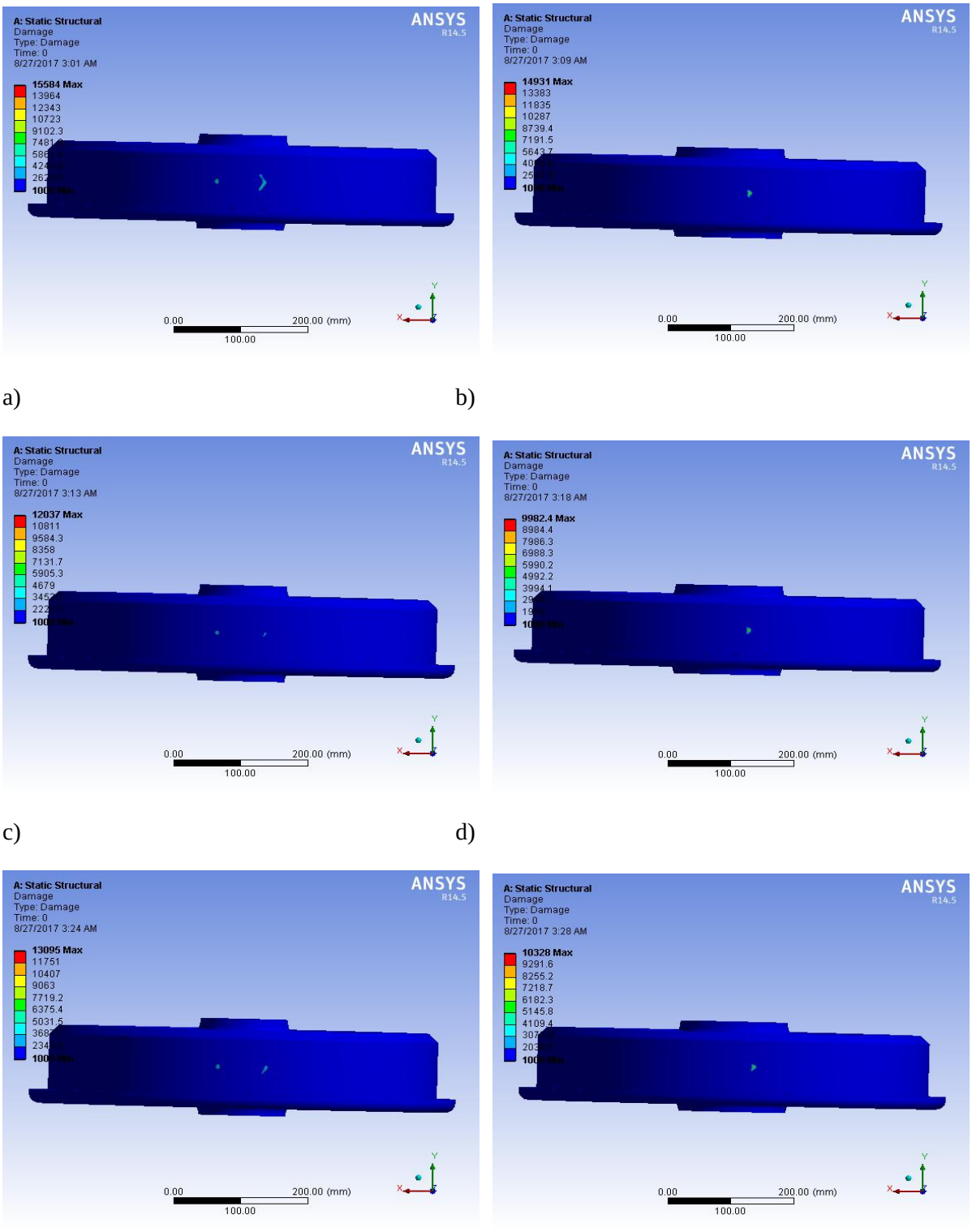

Figure 2: Fat. Damage a,c,e (R_2w 290) & b,d,f (R_2w 310) for CL60,ER7 & R8T wheels respect.

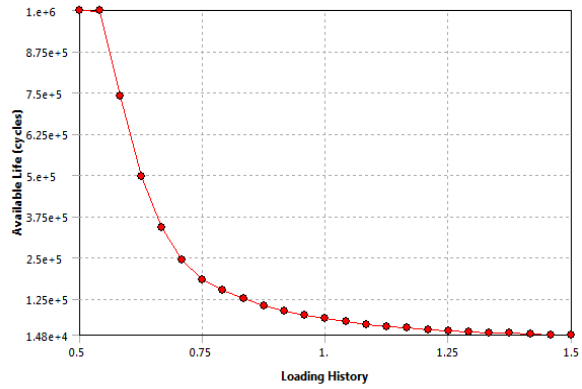

a)

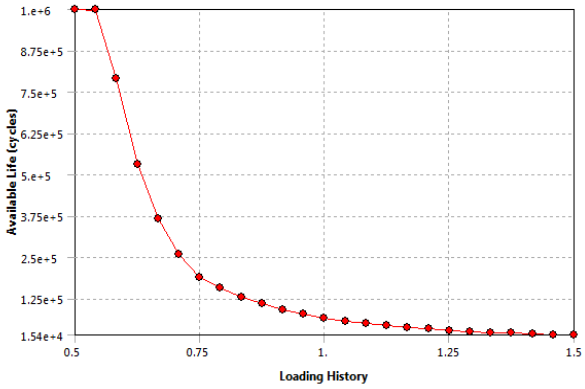

b)

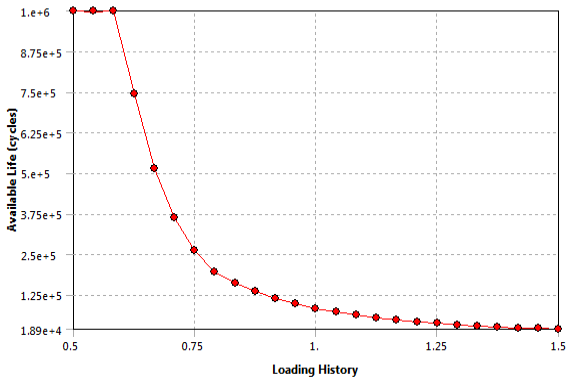

c)

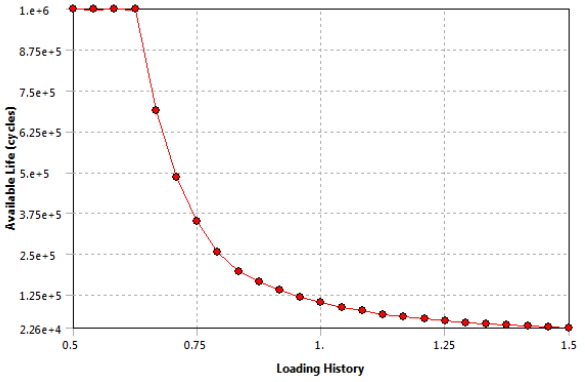

d)

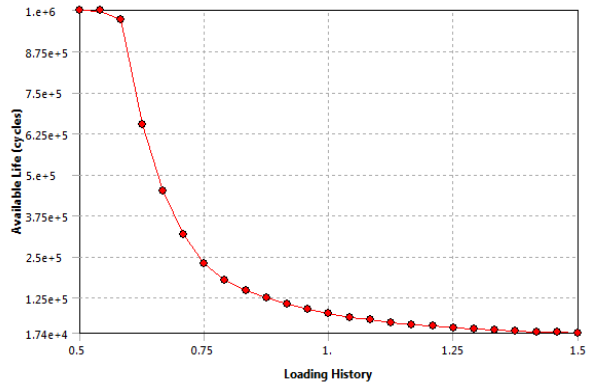

e)

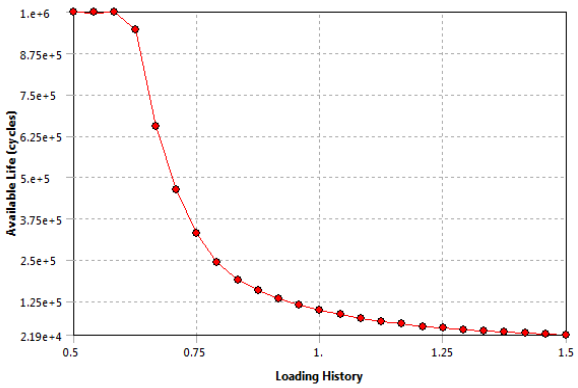

f)

Figure 3: Life vs Load a,c,e (R_2w 290) & b,d,f (R_2w 310) for CL60,ER7 & R8T wheels respect.

Table 1: Different wheel radiuses result summary

Wheel type	Applied load (N)	Wheel radius (mm)	Contact patches (mm)		Hertz coefficients		Stress (MPa)	Fatigue life (cycles)	Fatigue damage
			a	b	m	n			
CL60	54609	290	4.8	4.25	1.06	0.94	155.74	64,168	15,584
		310	5.015	4.161	1.0992	0.912	153.93	66,975	14,931
		330	5.2	4.1	1.13	0.89	148.58	76,262	13,113
ER7	54609	290	4.82	4.3	1.06	0.94	145.15	83,077	12,037
		310	5.05	4.21	1.0992	0.912	137.93	100,180	9,982.4
		330	5.3	4.13	1.13	0.89	130.3	123,140	8,120.7
R8T	54609	290	4.812	4.27	1.06	0.94	148.52	76,368	13,095
		310	5.038	4.18	1.0992	0.912	139.22	96,823	10,328
		330	5.23	4.12	1.13	0.89	136.13	105,060	9,518